STATIC ADSORPTION AND DYNAMIC RETENTION OF POLYACRYLAMIDES IN SANDSTONE RESERVOIR OF UZEN FIELD

by

RUSLAN KUSHEKOV

2021

Thesis submitted to the School of Mining and Geosciences of Nazarbayev University in Partial Fulfillment of the Requirements for the Degree of
Master of Science in Petroleum Engineering

Nazarbayev University
April 2021

ACKNOWLEDGEMENTS

I would like to express my dearest gratitude to my supervisor, Professor **Muhammad Rehan Hashmet**, for the unwavering support and thoughtful feedback throughout all stages of research. I appreciate your continuous support and guidance, which kept me motivated during the writing of this thesis. I acknowledge the opportunity you provided me to grow in this field of expertise.

I would like to extend my sincere thanks to my co-supervisor, **Professor Peyman Pourafshary**, for extended discussions and valuable suggestions. Without the persistent help of my supervisors, the goal of this project would not have been realized.

I would like to acknowledge the technical support of the **School of Mining and Geosciences and all its staff members** for providing excellent working conditions during the pandemic time. I thank my fellow **labmates and friends**, who have supported me for the past two years of study.

Last but not least important, I wish to acknowledge the support and great love of my **family**.

Originality Statement

I, Ruslan Kushekov, hereby declare that this submission is my own work and to the best of my knowledge it contains no materials previously published or written by another person, or substantial proportions of material which have been accepted for the award of any other degree or diploma at Nazarbayev University or any other educational institution, except where due acknowledgement is made in the thesis.

Any contribution made to the research by others, with whom I have worked at NU or elsewhere is explicitly acknowledged in the thesis.

I also declare that the intellectual content of this thesis is the product of my own work, except to the extent that assistance from others in the project's design and conception or in style, presentation and linguistic expression is acknowledged.

Signed on DATE

_____

ABSTRACT

In the context of the ending lifetime of the fields and unstable oil prices, Enhanced Oil Recovery (EOR) methods are particularly relevant. After primary recovery, waterflooding is the most common and economical practice to improve the oil recovery factor. At the current time, around 35% of the global average oil recovery factor is associated with waterflooding. However, the heterogeneity of formations and a great distinction between water and oil viscosities lead to fingering of the injected water leaving a large amount of oil untouched in the reservoir. According to estimation studies, around 7000 billion barrels of crude oil are remaining as residual oil after the secondary recovery phase. One of the oil fields where the tertiary recovery methods can be applied is the Uzen field, which is located in Western Kazakstan. Production rates at Uzen have been declining over the past decade and polymer flooding could make a significant difference. Among the technologies that can increase oil recovery, polymer flooding has significant advantages over other chemical methods, which are low risk and a wide range of applications. Despite the features of polymer flooding, a large amount of the injected polymer tends to adsorb on the rock surface whether it's sandstone or carbonate. The adsorption issue can limit the macroscopic sweep efficiency, and decrease the economic viability of the project. This study evaluates the adsorption properties of the acrylamide-based polymers by controlling their concentration and injection rate considering the conditions of the Uzen field such as formation type, water salinity and temperature.

The samples of Berea sandstone were used for the static and dynamic adsorption tests. A powder of the samples, which were obtained by core crushing, were mixed with the polymer solutions for the static test. Moreover, the polymer and sand mixtures were prepared with two liquid-solid ratios of 2:1 and 5:1. Three polymer types SAV 10, SAV 19, and SAV 10 XV with different concentrations were injected separately into the core samples for the dynamic adsorption test. The flowrates of 0.5, 1, 2, and 5 cc/min were applied during the coreflooding test. The polymer concentrations before and after adsorption were measured by the UV-vis Spectrophotometry device to estimate the adsorption levels for each polymer.

SAV 10 polymer was the first-priority polymer since it was selected for its rheological properties. Therefore, the static adsorption test was conducted for this polymer. As a result, it was observed that the increasing liquid-solid ratio negatively affect adsorption. Also, the high sensitivity of adsorption to mass concentration was noticed. Concerning mixing time, static adsorption increases smoothly during the first 10 hours, after that it reaches the equilibrium state between 24 and 48 hours.

No effect of flowrate on dynamic adsorption was observed during the injectivity test. SAV 19 polymer resulted in the lowest dynamic adsorption 320.97 mg/g, and SAV 10 XV demonstrated a quite similar result of 330.28 mg/g. The dynamic adsorption level of SAV 10 polymer resulted as 580.03 mg/g. The dynamic adsorption for SAV 10 polymer in the oil displacement test showed less value than it was in the injectivity test.

Table of Contents

LIST OF FIGURES

LIST OF TABLES

1 INTRODUCTION

1.1 Background

There are three main stages of oil recovery operations, which describe the production from a reservoir in a chronological sequence: primary, secondary, and tertiary. Primary recovery is the initial stage of production caused by innate forces inside of the reservoir. When natural energy is depleted, the production stage moves to secondary recovery. Secondary recovery implies pressure maintenance by flooding of water or gas into the reservoir. Tertiary recovery covers all the processes which are used to be conducted after waterflooding (or any secondary recovery processes). It includes the injection of chemicals, miscible gases, thermal energy, etc. to minimize residual oil quantity. These processes are methods of Enhanced Oil Recovery (EOR).

EOR processes are principally the injection of chemicals, gases, and applying thermal energy by using hot water or steam. Some of the gases which are used in EOR processes are carbon dioxide, nitrogen and hydrocarbon gases. Surfactants, polymers, and hydrocarbon solvents are chemicals that are commonly used in EOR. Injected fluids somehow change the reservoir and oil properties in situ, which allows to oil easily move to production wells. In other words, the fluids that are injected into the reservoir, interact with the rock and oil system, as a result, change this system to better conditions for oil displacement. For instance, using surfactants leads to a reduction of interfacial tension between oil and water while polymers make a piston-like front movement inside a reservoir. All interactions between injected fluids and the oil-rock system are based on chemical and physical mechanisms. The injection of water and dry gases are excluded from this description because they relate to immiscible displacement mechanisms.

Most of the field development plan is limited by waterflooding oil recovery method due to its low-cost operation and ease of use. This conventional waterflooding does not provide high ultimate oil recovery due to low water viscosity and high heterogeneity in the reservoir (Needham and Doe, 1987). The solution for occurred fingering problem can be the increase of water mobility by increasing the injected water viscosity (Mandal, 2015). The addition of water-soluble synthetic polymers or biopolymers tend to increase the viscosity of flooded water, hence the water/oil mobility ratio decreases and areal and vertical sweep efficiencies improve (Needham and Doe, 1987; Abidin et al., 2012; Sorbie, 2013; Mohsenatabar et al., 2018). The leading representative of synthetic polymers is partially hydrolyzed polyacrylamide (HPAM) (Sheng, 2010). A well-known representative of biopolymers is Xanthan, which is a high molecular biopolysaccharid (Katzbauer, 1998).

Figure 1 illustrates the waterfront of the conventional waterflooding and polymer flooding processes. There is a sign of early water breakthrough and ineffective macroscopic displacement due to viscous fingering in the first case of Figure 1. That scenario may occur when the mobility ratio is higher than 1 when the oil is heavy or due to reservoir heterogeneity. The second case illustrates that the viscosity of the injected water was improved by the addition of water-soluble polyacrylamide polymer (PAM), thus the time of water breakthrough was delayed, and the mobility ratio is equal to or below 1 causing almost piston-like displacement of oil. However, there is an effect of heterogeneity caused by high-permeable channel or large-scale layering.

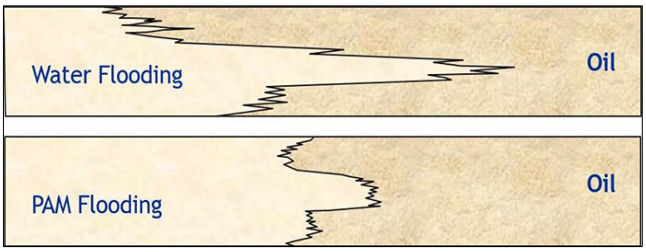

Figure 1. Waterflooding and polyacrylamide polymers (PAM) flooding displacement front (Thomas, 2016)

This technique is represented as polymer-augmented waterflooding or polymer flooding and can be injected as a slug or continuously (Speight, 2019). The application of polymers in the oil production process has been increased in recent time due to improved practical knowledge in this area. Several studies show that polymer flooding projects account for greater than 77% of chemical EOR (CEOR) projects worldwide (Rellegadla, 2017). Figure 2 demonstrates that most of the polymer flooding projects were applied in sandstone rocks due to the prevalent usage of anionic HPAM which can cause high adsorption on carbonates surface (Firozjaii and Saghafi, 2019).

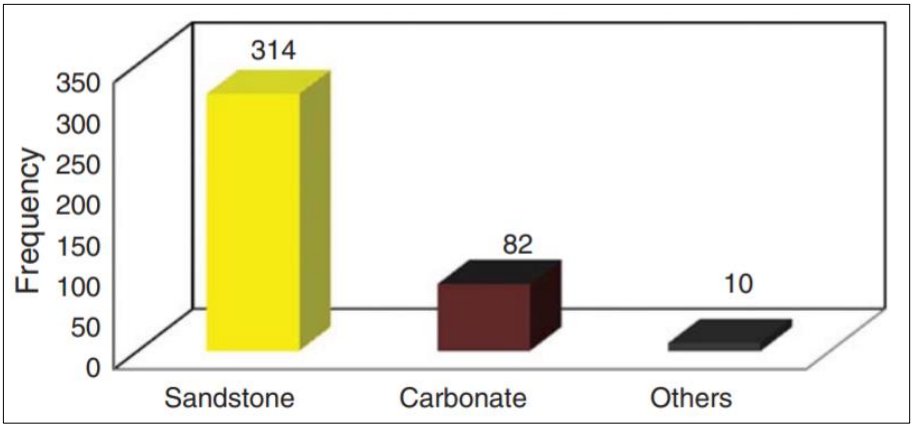

Figure 2. The lithology of polymer-flooding projects (Saleh, 2014)

The choice toward anionic polymers can be reasoned by numerous advantages. It has a higher viscosifying effect, more economically feasible to produce, and has a higher molecular weight comparing with cationic polymers. Cationic polymers are greatly shear sensitive and expensive to produce (Saleh, 2014).

There are several issues that may worsen the effectiveness of polymer flooding performance. There is a reduction in rock permeability and injectivity loss caused by polymer retention. For this reason, the issue of polymer retention requires further careful laboratory and field investigation. The thorough evaluation of polymer retention in porous media provides the success of the polymer flooding project (Al-Hajri et al., 2018). Mechanical trapping and adsorption are types of polymer retention in porous media. Low-permeability rocks are exposed to mechanical trapping of polymers due to pore size and channels distribution (Szabo, 1975; Willhite and Dominguez, 1977; Sheng, 2011). The interaction of rock surface and polymer molecules may result in polymer adsorption. This relationship strongly bonds the polymer molecules with the rock surface by van der Waal's and hydrogen bonding instead of chemisorption, thus the chemical bond between the polymer and solid surface scarcely forms (Hirasaki and Pope, 1974; Moffit et al., 1993; Mishra et al., 2014).

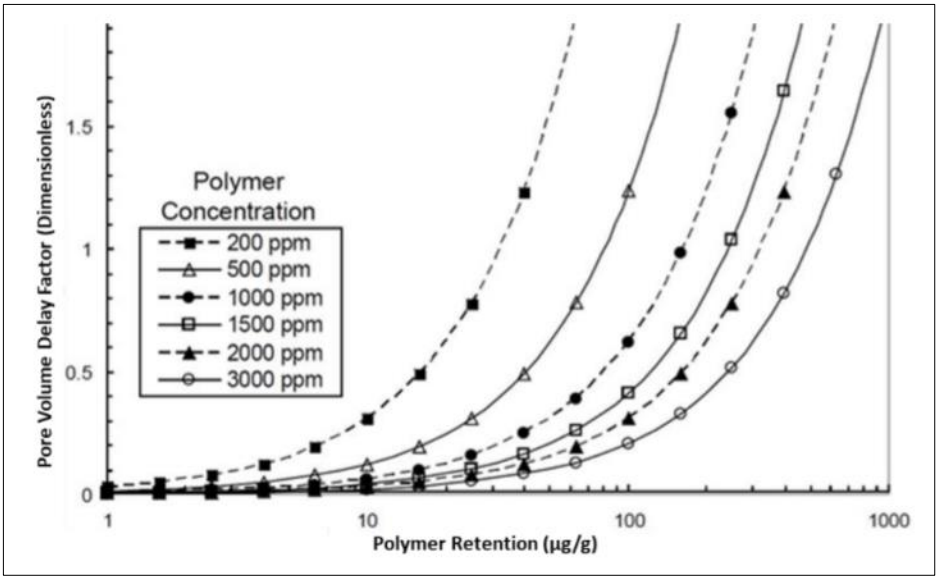

Figure 3. (Green and Willhite, 1998)

According to Figure 3, high values of polymer retention can strongly delay the oil movement and recovery. It can be noticed that at low polymer adsorption with a polymer concentration of 2000 ppm, the delay factor is 0.03-0.05 (3-5%), which means that compared with the ideal case where 0 polymer retention, 3-5% of more polymer required to be injected in order to reach the targeted formation (). For higher polymer retention of 100 µg/g, the pore volume delay factor

reaches 0.35 (35%). And when polymer retention will be 200 μg/g the economic feasibility and oil displacement efficiency of the polymer flooding project come into question.

1.2 Literature Review

1.2.1 Uzen oilfield characteristics

This section provides all the available latest data for the Uzen field, which were collected in the technical book written by Mullayev et al., (2017).

The Uzen field is located in the steppe part of Southern Mangyshlak and is administratively part of the Karakiya district of Mangistau oblast of Kazakhstan. The field was discovered in 1961, and after two years the first estimation of oil reserves was conducted. The initially estimated oil in place was observed as 8.400 million barrels (Sparke et al., 2005). The geology of the field is multi-bed with a complex structure of producing horizons and unique oil composition and properties. The main strata consist of 6 horizons containing 52 sandstone reservoirs with exceptionally high heterogeneity. The geological structure of the field is presented in two cross-sections in Figure 4.

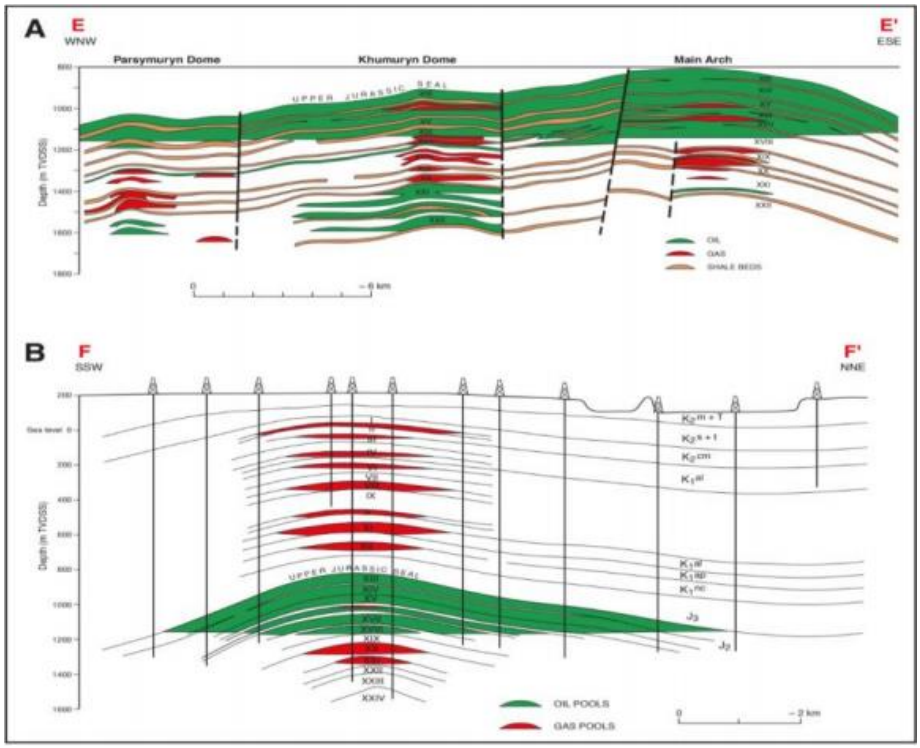

Figure 4. Geological structure of Uzen field: a) along the fold axis b) perpendicular to the fold axis (Ulmishek, 1990)

The geological section of the Uzen field has 26 sand horizons of Cretaceous and Jurassic deposits. Horizons I-XII (from top to bottom) of Cretaceous age are gas-bearing, horizons XIII-XVIII of Middle Jurassic age and are the main stage of oil and gas-bearing at depths from 1125 to 1334 m.

Hydrodynamic properties of the reservoir are presented in Table 1 for each horizon, where the average permeability varies from 79 to 523 mD. However, due to the high heterogeneity of the Uzen formation, it was decided to designate three technological Units in 2011. Unit 1 includes productive deposits with permeabilities of 300 mD and more. Unit 2 is considered as the medium permeable zone with values of 50-300 mD, and Unit 3 consists of permeabilities lower than 50 mD. The distribution of initial and current oil reserves by technological sub-objects of the Uzen field is shown in Table 2.

Table 1. Average physical properties of the reservoir

Horizon	Average porosity, %	Average permeability, mD
XIII	26.5	523
XIV	23.9	241
XV	23.3	173
XVI	22.0	79
XVII	22.8	232
XVIII	21.9	166

Table 2. The distribution of initial and current oil reserves by technological sub-objects

Technological Units	Oil initial in place, thousand tons	Cumulative oil production up to 2011, thousand tons	Residual oil reserves, thousand tons	Percentage of Unit residual oil reserves	Percentage of cumulative oil from initial reserves
Unit 1	164334	55293	109041	16%	33,64%
Unit 2	506028	218675	287353	43%	43,21%
Unit 3	315648	43329	272319	41%	13,72%
Total	986010	317297	668713	100%	32,17%

As can be seen from the data, the largest geological oil reserves are concentrated in Unit 2, and it provided the maximum oil produced. Unit 3 also has a significant residual oil share of about 41%. However, it has the worst production performance due to low permeable rocks.

A special feature of the oil of Uzen is its high paraffin content (up to 28%) and asphalt-resinous components (up to 20%). The detailed composition of the oil according to the latest data is presented in Table 3. Oil from productive horizons is known as highly viscous with an average value of 3.17-4.24 cp. The average density of oil is 0.768 gg/cc.

Table 3. The oil composition of the Uzen field for 01.01.2005

Horizon	**Components, % mol**											**Molecular weight, g/mole**
	CO_2	N_2	C_1	C_2	C_3	i-C_4	n-C_4	i-C_5	n-C_5	C_6	C_{7+}	
XIII	0.09	0.81	20.99	8.98	8.06	1.99	3.77	1.99	2.11	4.32	4.31	195
XIV	0.11	0.66	22.85	8.50	6.79	1.60	2.88	1.82	2.19	5.49	5.94	190
XV	0.09	0.30	27.13	8.18	5.69	1.48	2.79	1.33	1.76	2.52	2.45	188
XVI	0.08	1.18	25.35	6.89	4.64	1.15	2.18	2.11	2.44	6.10	6.68	199
XVII	0.06	0.38	22.42	8.45	5.85	1.27	2.56	1.71	1.52	5.78	8.59	193
XVIII	0.06	0.41	23.98	9.01	6.19	1.33	2.64	1.69	1.50	5.55	8.18	192

The lack of a pressure maintenance system at the start of field development led to reservoir degassing in areas of intense drainage by 1967. This led to a drop of reservoir pressure below bubble-point pressure and the development of a dissolved gas regime. Therefore, it was decided to start water injection to maintain reservoir pressure. Active water injection for pressure maintenance purposes has led to watering of the reservoir and, consequently, to changes in the physicochemical and rheological properties of the reservoir fluid. Studies of downhole oil samples from this period showed that, compared with initial oil characteristics, bubble-point pressure and gas content decreased, while density and viscosity increased. In 1972, the injection of hot water was successfully tested and started to reduce paraffin precipitations in the gathering system. The water injection history with its efficiency is presented in Figure 5.

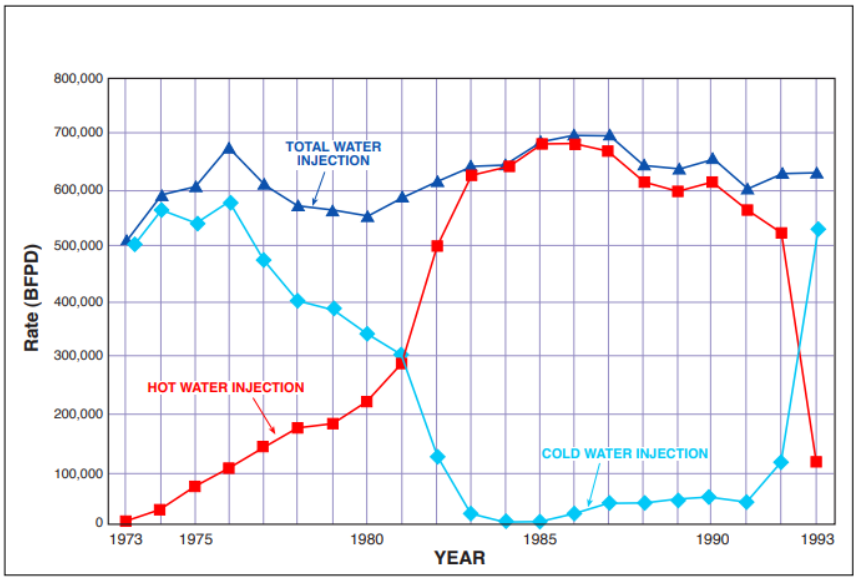

Figure 5. Water injection history of the Uzen field, 1973-93 (C & C Reservoirs, 2010)

Accordingly, from 1967 till the current time the injection of water is the method of oil recovery, which ended up with high water-cut. The latest average water-cut value measured in 2014 is 86%, as shown in Figure 6.

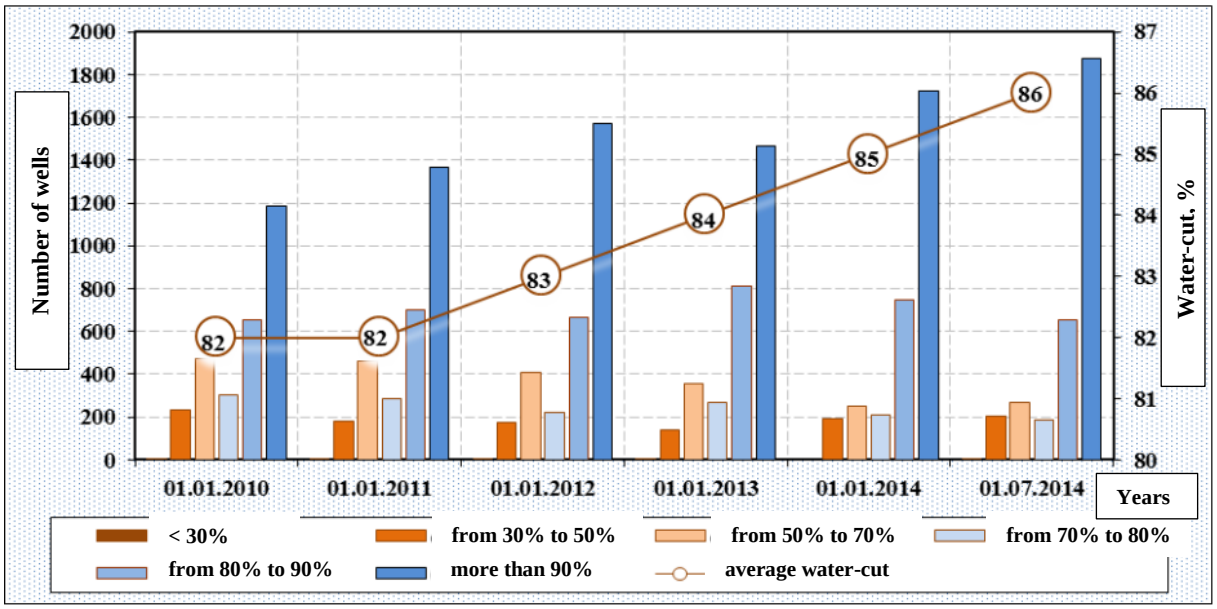

Figure 6. Dynamics of average water-cut of wells on XIII-XVIII horizons of the field, 2010-14 (C & C Reservoirs, 2010)

Table 4 demonstrates the ion composition of formation and injected water. According to the table, the maximum concentration of formation water is 77000 ppm and consists mainly of monovalent particles. Therefore, the application of HPAM based co and ter-polymers could be appropriate, since the monovalent particles are less crucial for them (Sheng, 2011).

Table 4. Ion composition of formation/injected water of Uzen field (Research and Design center “Nedra” LPP)

Water type	Components, mg/l						Mineralization, g/l	pH	Density, g/cc
	Ca^{2+}	Mg^{2+}	Na^{+}+K	Cl^{-}	SO_4^{2-}	HCO_3^{-}			
Marine	450	780	3861	6390	3360	250	15.09	7.0	1.009
Volzhskaya	44	14.4	190.8	255	150	83	0.73	7.0	1.000
Wastewater	3000	900		31950	1200	458	51.4	6.5	1.036
Formation water:									
XIII	3237	1088	17599	35241	715	440	58	-	1.037
XIV	3220	1140	17034	34538	668	420	56	-	1.037
XV	4231	1230	21763	43788	950	221	72	-	1.046
XVI	4448	1300	23426	46731	832	350	77	-	1.049
XVII	3199	900	17663	34711	770	398	57	-	1.037
XVIII	4364	1200	23567	46573	1020	380	77	-	1.048

Uzen oil production peaked in 1975 at 320,000 bopd. Production then gradually declined to 50,000 bopd in 1996, with a corresponding reduction in active production wells and surface facilities. The production history of the field till 2005 is shown in Figure 7.

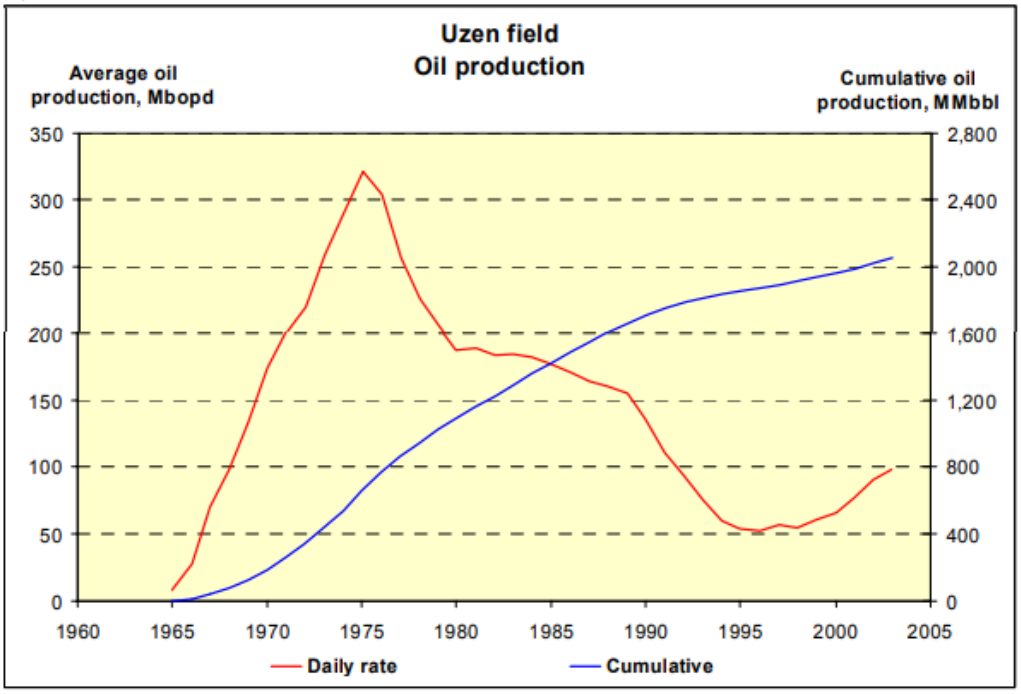

Figure 7. Uzen oil field production history (Sparke et al., 2005)

As shown in the graph, there was a slight increase in oil production in 1980. This increase is caused by implemented tertiary recovery technique – surfactant flooding. The concentration of surfactant was 0.05% wt and it was flooded into XIII and XIV horizons, which belong to high-permeable Unit 1. Moreover, during the surfactant injection period, a number of geological and engineering operations were carried out in the field:

- intensive drilling of new production wells;
- spot waterflooding since 1978;
- reconstruction of the formation pressure maintenance system, which has enabled a significant increase in injection volumes;
- full transition to hot water injection (thermal EOR) from 1988.

All of these activities were carried out at the same time as the surfactant injection pilot works, which makes it very difficult to assess the impact of each of the above activities on improving the development status of the pilot sector. However, it was approximated that incremental oil for the period of surfactant flooding is 633 thousand tons (83.4%). As already stated, surfactant flooding was implemented in Unit 1, which has high permeability of over 300 mD. Therefore, the viscous fingering was figured out during surfactant flooding, which led to high water-cut in production wells.

According to all the presented data, the Uzen field has faced two crucial problems – viscous fingering and high water-cut. Therefore, it can be assumed that a solution to these problems can be realised by polymer flooding as a tertiary recovery method. Polymer flooding which improves the sweep efficiency by a decrease in mobility ratio helps to overcome viscous fingering and thereby high water-cut (Sheng, 2011).

1.2.2 Polymer Flooding

Polymers are used to overcome the problem of high mobility ratio by increasing the viscosity of displacing fluid. The decrease in the mobility ratio helps to improve sweep efficiency and increase oil production by providing a stable displacement flow (Al-Abri, et al., 2012). Mobility control at favourable conditions may significantly enhance the effectiveness of oil production.

Injection of polymer helps to increase the viscosity of displacing fluid and to decrease the mobility ratio. The problem with unfavourable mobility ratio can be solved using polymer flooding (Qi, et al., 2017). Polymers can be characterized as a chemical compound with a large

molecular structure that is formed by repeated small compounds bonded together through a polymerization reaction (Carraher, 2017).

There are two commonly used types of polymer: synthetic and biopolymers. As the name says, synthetic polymers are synthesized artificially, and biopolymers are made from natural products. The most recognized synthetic polymer is hydrolyzed polyacrylamide, and a biopolymer is xanthan gum. Polymers such as guar gum, hydroxyl ethyl cellulose (HEC), and sodium carboxymethyl cellulose are not widely used. Table 5 shows the typical features of certain polymers.

Table 5. Polymer structures and their characteristics (Zhao, 1991)

Structure	Characteristics	Sample Polymers
-O- in the backbone	Low thermal stability, thermal degradation at high T, only suitable at <80º C	Polyoxyethylene, sodium alginate, sodium carboxymethyl cellulose, HEC, xanthan gum
Carbon chain in the backbone	Good thermal stability, degradation not severe at <110°C	Polyvinyl, sodium polyacrylate, polyacrylamide, HPAM
–COO− in hydrophilic group	Good viscosifier, less adsorption on sandstones due to the repulsion between chain links, but precipitation with Ca^{2+} and Mg^{2+}, less chemical stability	Sodium alginate, sodium carboxymethyl cellulose, HPAM, xanthan gum
–OH or –CONH2 in hydrophilic group	No precipitation with Ca^{2+} and Mg^{2+}, good chemical stability, but no repulsion between chain links, thus less viscosifying powder, high adsorption due to hydrogen bond formed on sandstone rocks	Polyvinyl, HEC, polyacrylamide, HPAM

An acceptable polymer supposed to have the following properties (Sheng, 2010):

- Good viscosifying powder
- Negative ionic hydrophilic group for the reduction of adsorption on rock surfaces
- Nonionic hydrophilic group for chemical stability
- No –O– in the backbone (carbon chain) for thermal stability

HPAM-based polymers were used for the evaluation of the applicability in the Uzen sandstone reservoir. According to geological data of the field, it can be stated that polymers should be tested under harsh conditions such as high salinity of 77000 ppm, high temperature around 58^0-63^0 C, and highly viscous oil of 3.14-4.22 cp. Unfortunately, HPAM polymers display poor behaviour in the presence of divalent cations and temperatures above 60^0 C. In such conditions the rate of hydrolysis accelerates, resulting in the precipitation of polymer molecules (Zaitoun et al., 1983; Moradi-Araghi, 1987; Seright et al., 2010; Levitt and Potie, 2011). Moreover, the presence of oxygen can lead to a strong degradation of polymer solutions (Seright et al., 2010). As synthetic polymers are cheaper and easy to adjust, they are more closely scrutinised. Therefore, the use of synthetic polymers is more common in the literature than biopolymers. One of the methods of improving polymers behaviour under harsh conditions is functionalizing them with monomers resulting in new co- and terpolymers that are more stable thermally and chemically. Table 6 provides the most common monomers that can be applied in harsh conditions.

Table 6. Chemistry of different monomers used to functionalize acrylamides (Waleed et al., 2019)

Monomer	Chemical Name	Charge	Main Function
AM	Acrylamide	Nonionic	The main constituent of synthetic EOR polymers
PAM	Polyacrylamide	Nonionic	Hydrolyzed form of polyacrylamide
HPAM	Partially Hydrolyzed Polyacrylamide	Anionic	The partially hydrolyzed form of polyacrylamide
AA	Acrylic acid	Anionic	Limits hydrolysis and thermal degradation, also a product of AM hydrolysis
AMPS	2-Acrylamido-2-MethylPropane-Sulfonate	Anionic	Increases tolerance to salinity
ATBS	Acrylamide-Tertio-Butyl Sulfonate	Anionic	Limits hydrolysis and thermal degradation
NVP	N-Vinyl-Pyrrolidone	Nonionic	Limits hydrolysis and thermal degradation

1.2.3 Polymer Retention

Adsorption, hydrodynamic retention, and mechanical trapping are mechanisms that are associated with polymer retention. Willhite and Dominguez (1977) first have described these terms. Hydrodynamic retention and mechanical trapping appear only in dynamic conditions, i.e. flow in porous media. They don't have any meaning in powder solution experiments.

Willhite and Dominguez (1977) have stated that the mechanism when large molecules of polymer trapped in relatively small pore throats are called mechanical entrapment.

Chauveteau and Kohler (1974) have experimented and proved that polymer retention level increases by increasing the injection rate. This form of retention based on the rate is called hydrodynamic retention, which is not explained properly yet. However, as Sorbie (1991) provides, this type of retention has not a big contribution to the overall retained polymer amount.

Regarding adsorption, it relates to interactions between rock surface and molecules of polymer. Polymer molecules bound to the rock surface because of hydrogen bonding and van der Waals forces. The rock surface is covered by polymer molecules. It is obvious that this process reduces formation permeability and there is the only way to separate polymer from bulk solution, is by adding some solid powder, such as latex beads and silica sand, into the bulk solution until it reaches equilibrium.

There are two types of adsorption: physical adsorption and chemisorption. Chemisorption occurs when the chemical bond formation between sorbate and adsorbent is taking place. Physical adsorption is characterized by weak intermolecular forces between polymer and rock surface. The adsorption of polymer in porous media is caused by physical adsorption as shown in Figure 8. The physical adsorption is supposed to be reversible, but the polymer adsorbs in multiple sites on the surface of the rock, because of the large size of the polymer molecule. Therefore, many authors (Lakatos et al. 1979; Szabo 1979; Gramain and Myard 1981; Zhang and Seright 2014) reported that polymer adsorption is irreversible.

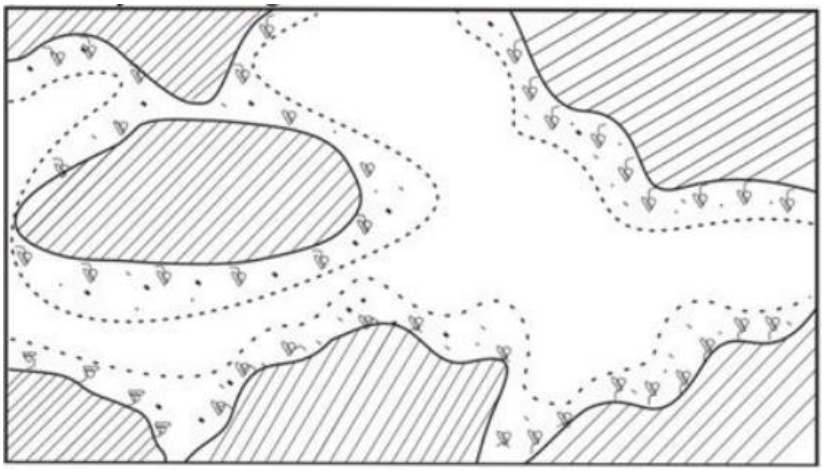

Figure 8. Polymer adsorption in porous media

The conformation of the adsorbed macromolecule can be influenced by the size of the polymer molecule because the polymer molecule segments don't adsorb on the rock surface at the same time. Figure 9 presents the conformation which usually consists of tail, loops, and trains.

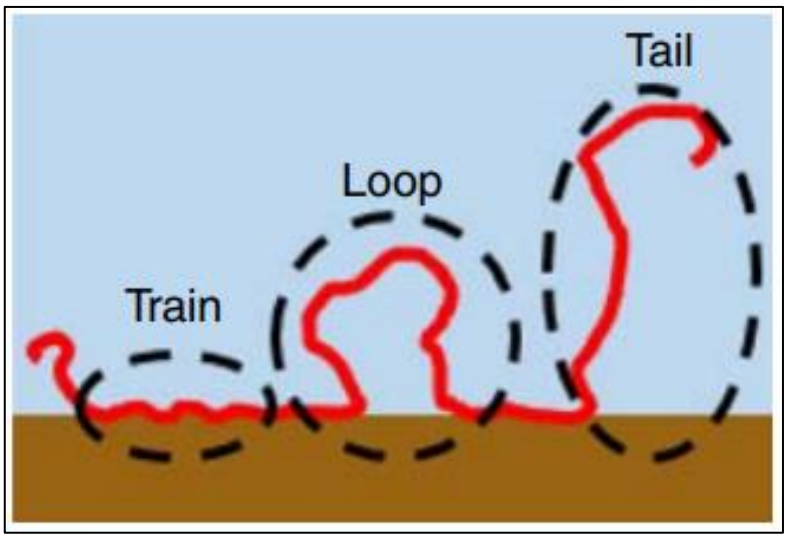

Figure 9. Schematic of the polymer-molecule conformation (Goddard and Gruber 1999)

To avoid or decrease mechanical entrapment several procedures should be conducted. For example, it can be pre-shearing or pre-filtering of the polymer solution. In the case of high permeable formations, mechanical entrapment is expected to be less. Concerning hydrodynamic retention as mentioned before it does not have such a big contribution and significance (Sorbie, 1991). Therefore, this term can be neglected. The most important mechanism among these three is adsorption because it is a basic property of the polymer/rock surface system. The retention of polymers is more meaningful in comparison to surfactants and alkalines. Nevertheless, it is problematic to differentiate these three mechanisms, therefore the term adsorption is used to describe all of them.

There are many chemical and physical properties of injected agents and rock surface that affect polymer adsorption. Many laboratory studies reported the impact of polymer, fluid, and rock characteristics on the adsorption and retention capabilities of polymers. These factors are summarized in Figure 10.

Szabo conducted an experiment on Berea sandstone cores to measure the adsorption level for different types of polymers, including HPAM-based, bio, and other polymers. Biopolymers retained the lowest value of measured retention, followed by 2-acrylamido-2-methyl propane sulfonate (AMPS) and HPAM (Szabo, 1975). Figure 11 illustrates the difference in adsorption for different types of polymer.

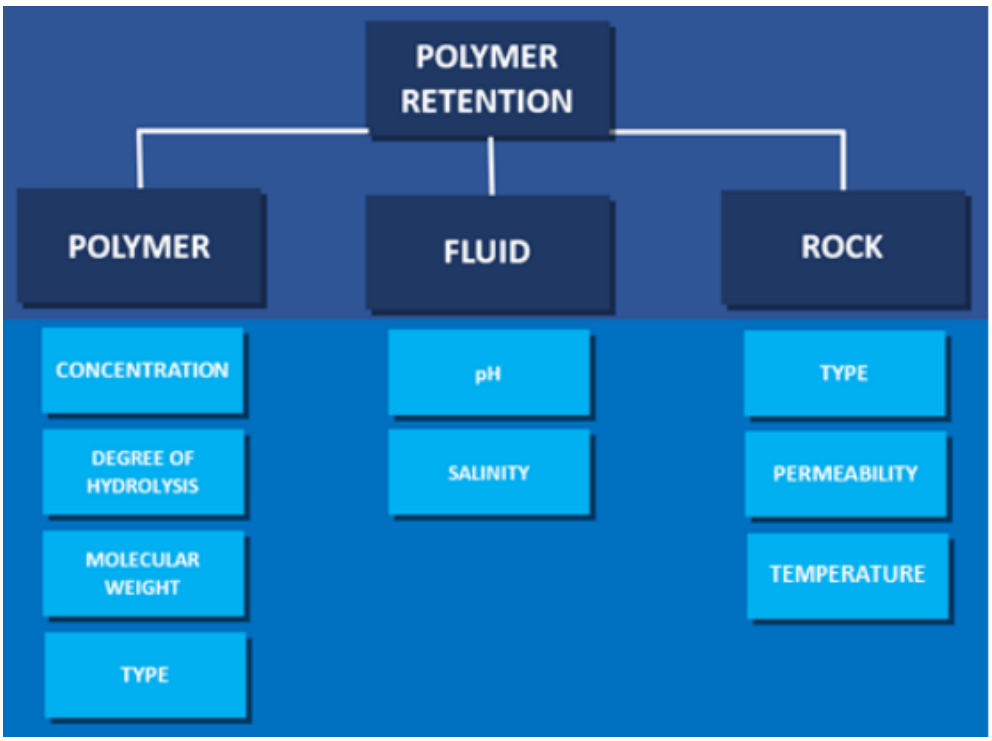

Figure 10. Factors that affect polymer retention

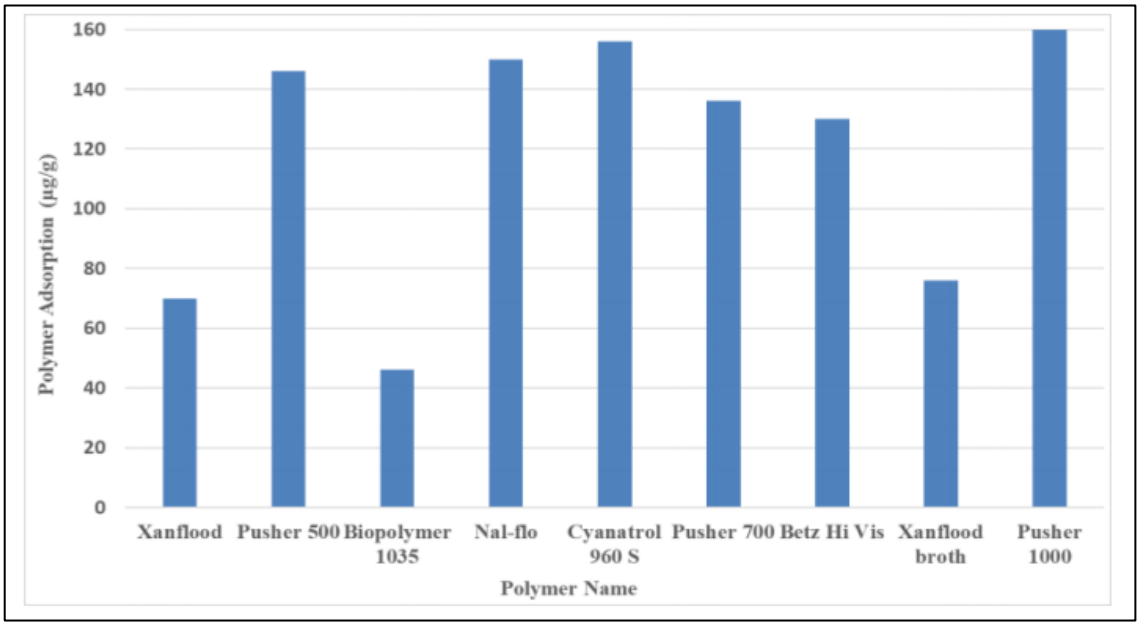

Figure 11. Polymer absorption as a function of the type of the polymer (Szabo, 1975)

The pore size distribution is the main factor affecting mechanical trapping. Mechanical entrapment occurs often in reservoirs with low permeability (Szabo, 1975). Near zone of injection wellbores can be plugged and damaged, if the entrapment process occurs in up to average pore sizes. It leads to the exponential penetration of polymer solution into the formation. The reservoir permeability should be examined foremost because these criteria cannot be regulated during the flow of fluids. For the benefit of polymer flooding, the pore size and permeability is a key factor for the economic success of the project due to the high cost of

the polymer. These parameters should be sufficiently large to prevent pore blockage. Polymer retention significantly increases with the decrease of pore size and permeability (Rellegadla et al., 2017). Table 7 shows the variations of rock type and permeability on the retention.

Table 7. The dependency of rock type on retention

Rock Type and Permeability	Polymer Type	Retention (μg/g)
Vosges sandstone 2100 md	HPAM	155
Vosges sandstone 520 md	HPAM	140
Reservoir sandstone 137 md	HPAM	12
Reservoir sandstone 12 md	HPAM	130

Another extensive studies showed a straight dependence of polymer properties such as concentration, molecular weight and degree of hydrolysis on polymer retention (Willhite, 1988; Huang & Sorbie, 1993; Zheng et al., 1998; Rashidi et al., 2009; Lakatos et al., 1981). All these studies claimed that polymer retention increases with the increase of these characteristical features regardless of the polymer type. The results of the dependency of polymer adsorption on concentration are summarized in Table 8. The degree of hydrolysis is proportional to the temperature. Consequently, the increase of temperature increases the negative charge on the rock surface and degree of hydrolysis by converting of amide groups to negatively charged carboxylic groups. As a result, the electrostatic repulsion between the carboxylic group and the rock surface leads to a decrease in polymer retention (Sheng, 2010).

Table 8. Polymer concentration effect on retention

Polymer Concentration (ppm)	Type of Polymer	Retention (μg/g)
10–6000	HPAM	20–420
20–1000	HPAM	21–30
250–1500	HPAM	40–58
50–200	Scleroglucan	8.2–11.7

1.2.4 Experimental studies on static and dynamic adsorption of polymers

Ferreira and Moreno (2020) have done extensive work on the adsorption of polymers in sandstone porous media. The authors divided the adsorption types according to Brunauer et al. (1940) and made a huge review on papers related to polymer adsorption. Based on Brunauer classification, the physical adsorption of polymers can be divided into 5 Langmuir type isotherms, as shown in Figure 12.

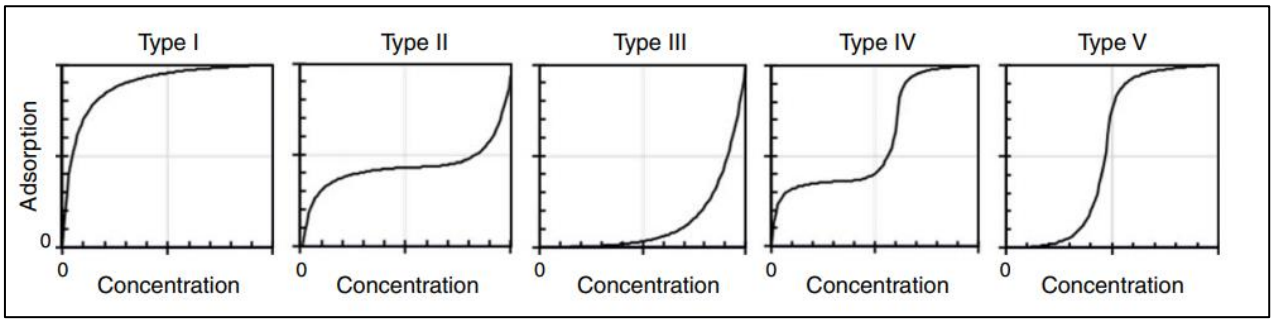

Figure 12. Qualitative examples of the five types of physical adsorption isotherms (Brunauer et al., 1940)

Commonly, these types of adsorption are used in large-scale EOR applications (Lakatos et al. 1979; Sheng 2011; Dang et al. 2014). However, some laboratory observations motivate the modelling based on Langmuir isotherms (Ali and Mahmud 2015; Quadri et al. 2015; Li et al. 2016), even though many authors conducted experimental works on the adsorption of polymers in virgin porous media deviating from the Langmuir isotherm. Lee and Somasundaran (1989) studied the adsorption of a nonionic polyacrylamide on minerals such as Fe_2O_3, Cr_2O_3, Al_2O_3, TiO_2, SnO_2, and SiO_2 and built Langmuir isotherms for different pH values. Also, these isotherms were obtained on a static adsorption test conducted by Argiller et al., (1996). The authors investigated the adsorption values of polyacrylamides on different minerals such as montmorillonite and siliceous materials. However, not all the polymers follow the Langmuir isotherms. For instance, Deng et al. (2006) tested several polymers on smectite, illite, and kaolinite and observed that cationic polyacrylamides do not follow isotherms as shown in Figure 13.

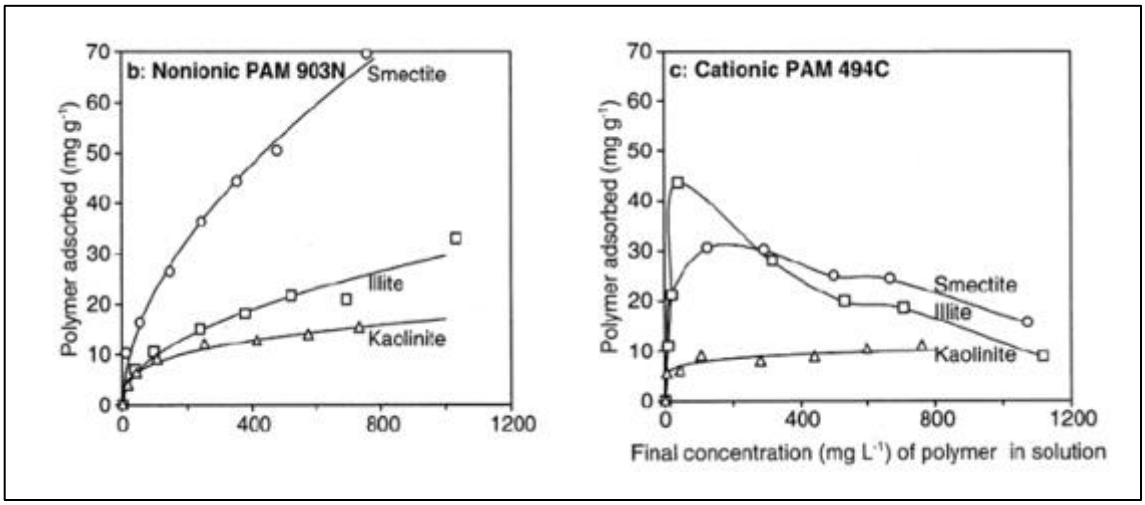

Figure 13. Polymer isotherms (Deng et al., 2006)

1.2.4.1 Adsorption on different minerals

Quadri et al., (2015) conducted a static adsorption test for biopolymer Schizophyllan on several minerals of carbonate and sandstone such as calcite, dolomite, kaolin, and silica. The methodology of measuring adsorption was an analyzing the surface chemistry of minerals via X-Ray Photoelectron Spectroscopy. Also, the measuring procedure was carried out considering the reservoir brine temperature of 70^0C. Figure 14 represents the static adsorption on different minerals.

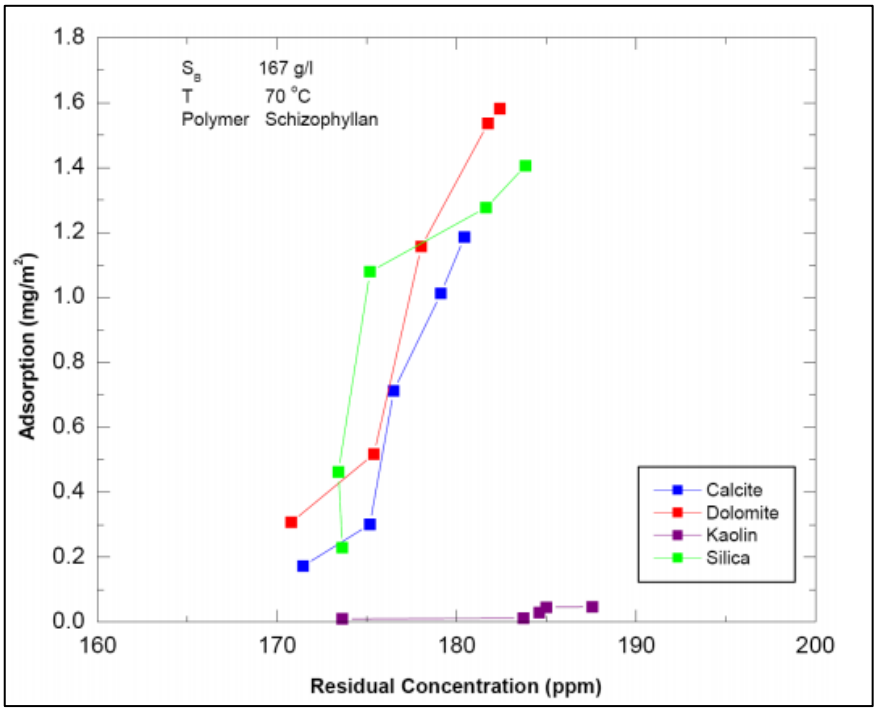

Figure 14. Adsorption on different minerals (Quadri et al., 2015)

As shown in the graph, the adsorption levels for calcite, dolomite, kaolin, and silica was 1.18, 1.58, 0.046 and 1.40 mg/m^2 respectively.

1.2.4.2 Effect of brine salinity

Further, the authors have investigated the effect of salinity on adsorption level over calcite. Three salinities of 0%, 50% and 100% were applied in this test. As depicted from the results, the static adsorption level tends to decrease with an increasing water salinity as shown in Figure 15.

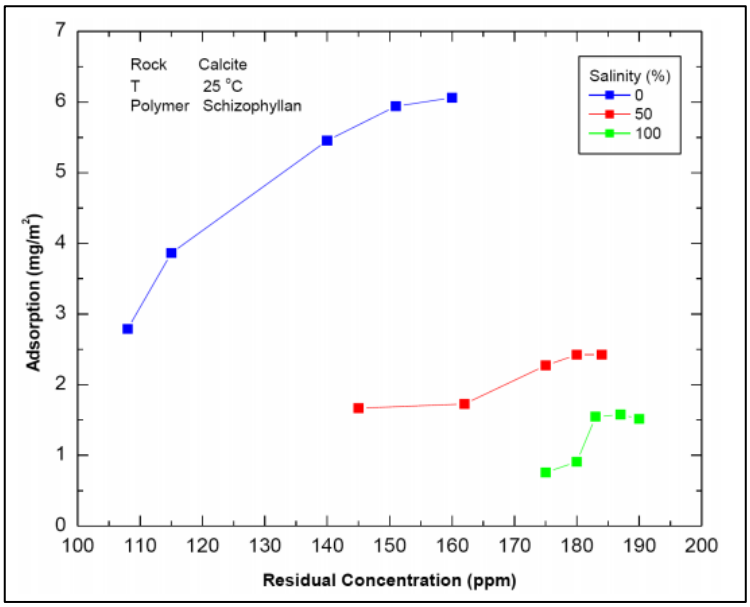

Figure 15. Effect of salinity on adsorption of Schizophyllan on calcite (Quadri et al., 2015)

The same experiment was conducted for all minerals. It was noticed that the adsorption for all minerals is decreased when salinity is increasing. However, the magnitudes for kaolin and silica are not the same as it was observed for calcite and dolomite. This may be attributed to the different interactions of Schizophyllan with mineral ion and/or kosmotropic properties of the background ions.

1.2.4.3 Effect of temperature

The effect of temperature was also investigated by Quadri et al. (2015). The same mineral calcite was used for the static adsorption test at two different temperatures of 25^0C and 80^0C. The adsorption decreased from 1.2 to 0.84 mg/m^2 as shown in Figure 16.

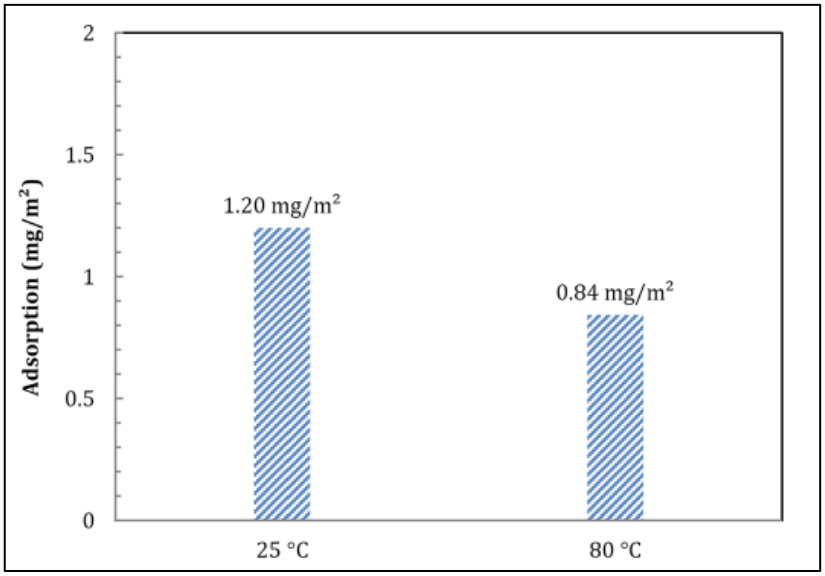

Figure 16. Effect of temperature on adsorption of Schizophyllan on calcite (Quadri et al., 2015)

This is the typical polymer behaviour regarding temperature changes as it was described by Hollander et al. (1981).

Similar studies on the effect of temperature on adsorption were also provided by Li et al. (2016) as shown in Figure 17. It is worth mentioning that the static and dynamic adsorption tests were carried out on Viscoeloastic Surfactants (VES), which are promising flooding agent in recent years. This chemical enables to not only reduce the oil-water interfacial tension but to control the mobility ratio as polymers. It is obvious that the observed values of the paperwork cannot be compared with the measurements of this thesis. However, the methodology which is used during this study can be considered appropriate to implement in polymer adsorption tests. The UV spectrophotometer was used for establishing a standard calibration curve for VES and determining solution concentrations.

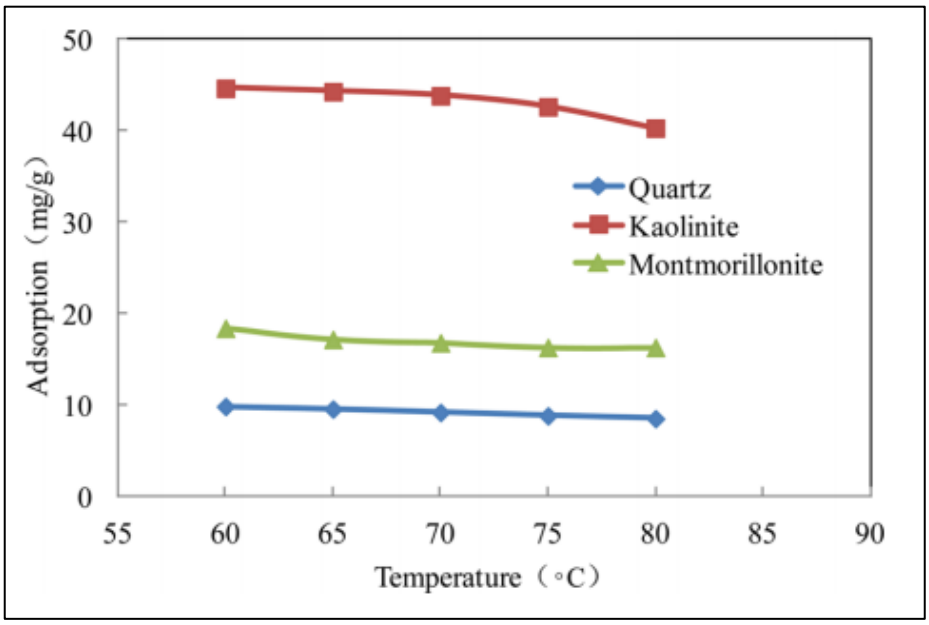

Figure 17. VES adsorption as a function of temperature (Li et al., 2016)

1.2.4.4 Effect of concentration and time

After a year Li et al., (2017) have studied the static and dynamic adsorption of polymers A, B, C on sandstone rock and obtained the isotherms of adsorption as a function of concentration. The static adsorption test was conducted using a crushed 40-90 mesh sand grain. The sand was soaked in petroleum ether for 12 hours and then was heated in an oven over 24 hours at 120^0C. The UV spectrophotometer was also used for determining UV absorbance before and after the adsorption test. As a result, it has been recognized that the adsorption of the used polymer was very sensitive to mass concentration. It was observed that the static adsorption increased with

polymer concentration until the plateau is reached as shown in Figure 18. Under their experimental conditions, the highest adsorption level was around 22 mg/g for polymer A.

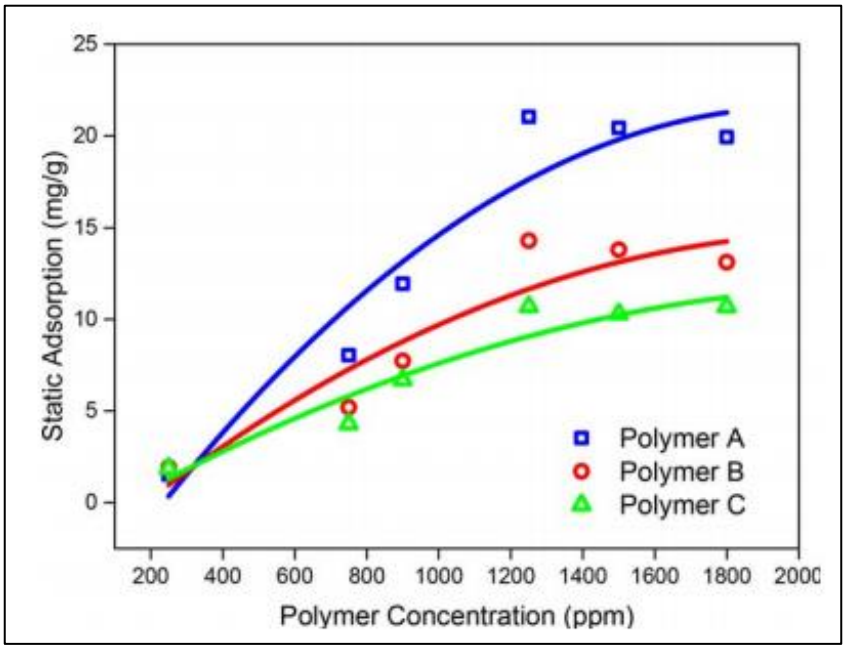

Figure 18. Static adsorption of the polymer as a function of concentration (Li et al., 2017)

Figure 19 plots the static adsorption depending on mixing time. It was noticed that the magnitudes of all three polymers gently increased to the peaking value and then slightly dropped in about 20 hours. This is an indication of multilayer adsorption, which is more pronounced when polymers with high molecular weight are used. Some polymer chains might be unlocked between 20 and 25 hours, therefore the adsorption value drop was obtained.

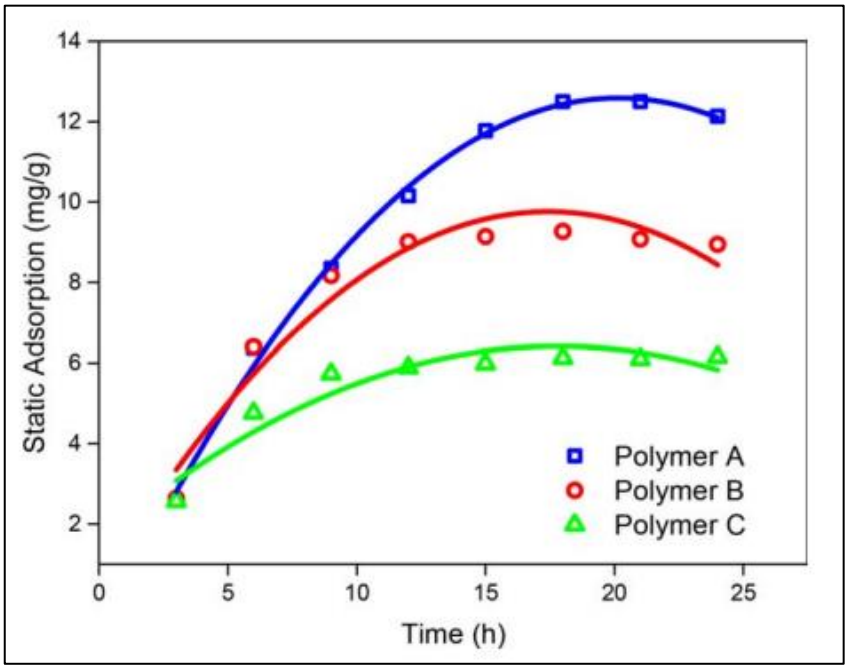

Figure 19. Static adsorption of the polymer as a function of time (Li et al., 2017)

1.2.4.5 Effect of liquid-solid ratio

Also, the effect of the liquid-solid ratio and time during the static test has been studied during this study. Li et al., (2017) were the first who established such kind of methodology to evaluate static adsorption. The authors have observed that the adsorption levels of all three polymers are smoothly increased with the factor of liquid-solid ratio until the value of 30:1 as shown in Figure 20. This can be attributed that the equilibrium adsorption state between sand and polymer has achieved. Further, the ratio where the constant adsorption value begins should be used throughout the next static adsorption tests.

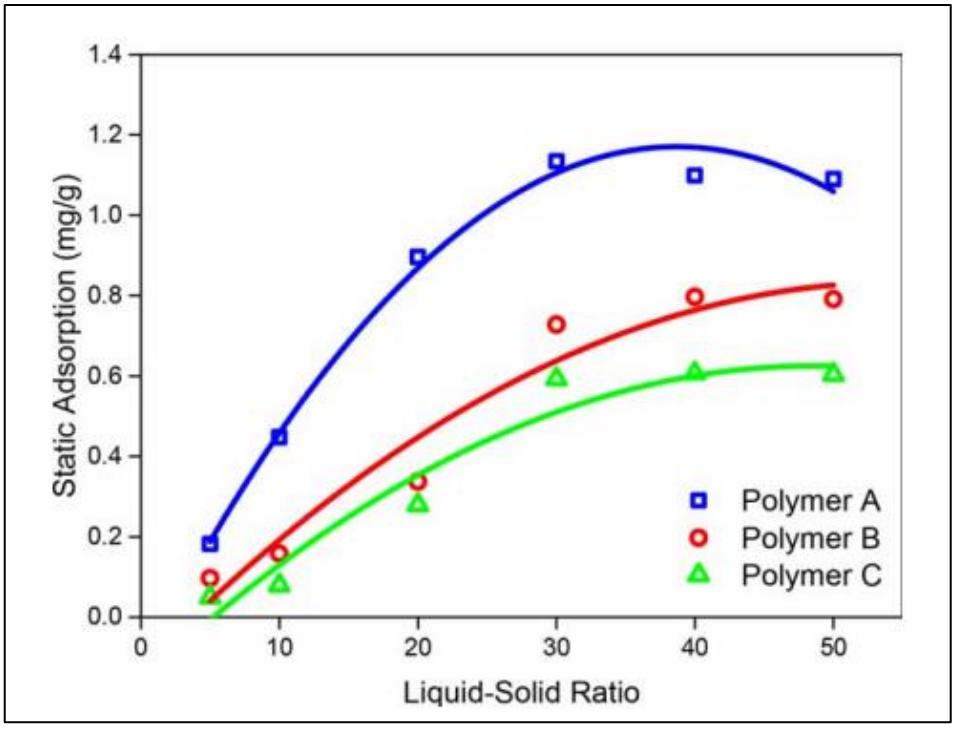

Figure 20. Static adsorption of the polymer as a function of liquid-solid ratio (Li et al., 2017)

1.5 Problem definition

Despite the fact that polymer flooding was successfully implemented over decades of years, the problems with penetration into porous medium are still exist. One of the main problems is polymer adsorption and retention which can cause permeability reduction in the formation and loss of injected water viscosity. Fluids that are injecting lose flowability, especially in low permeable rocks.

The analysis of studies done on polymer injection shows that loss of polymer in the porous medium is an important issue that has not been studied extensively. Loss of polymer due to adsorption is one of the influencing factors during polymer injection that provides the best

mobility control. Properly selected polymer type and its concentration can provide a technically and economically successful polymer flooding project. In this study, the HPAM-based polymers SAV 10, SAV 19, and SAV 10 XV were tested in terms of adsorption properties considering the Uzen field parameters. Thus, the temperature of 60^0 C was applied during the injectivity and oil displacement test. The target viscosity of polymer solution was adjusted as a 4 cp similar to the viscosity of Uzen's oil to achieve an appropriate mobility ratio. Based on target viscosity and thermal degradation, the concentrations for each polymer were obtained. The use of Berea samples was the only assumption, which can be related to the Uzen sandstone reservoir for conducted experiments.

1.6 Objectives of the Thesis

1.6.1 Main Objectives

According to the problem statement, the following objectives should be accomplished to estimate the adsorption characteristics of the proposed acrylamide-based polymers:

- Analyzing the different methodology for designing the proper adsorption tests for proposed polymers;
- Investigating the effect of liquid-solid ratio (LSR), mixing time and concentration on static adsorption of polymers on crushed sandstone;
- Performing the injectivity test to check the dynamic adsorption of polymers on sandstone core samples with and without the presence of oil;
- Investigating the effect of flowrate and concentrations during the dynamic adsorption test.

1.6.2 Thesis structure

Chapter 2 describes the necessary materials and their preparatory stages for laboratory experiments that contribute to the estimation of polymer adsorption. The list of necessary materials includes the following: core samples, crushed core, brine, polymers. Also, this section provides information about the required types of equipment and a step-by-step working methodology. The main procedures of the experimental study include sand, brine and polymer solution preparation, static and dynamic adsorption tests.

Chapter 3 analyzes and reveals the data obtained by experiments. This chapter includes graphs and calculations that evaluate the adsorption properties of the proposed acrylamide-based polymers. Moreover, this section points out the effect of concentration of polymer, mixing time and liquid-solid ratio on polymer adsorption.

Chapter 4 concludes the important points of the study and issues the research development options.

Chapter 5 provides the list of references that were used during the study.

2 METHODOLOGY

Laboratory experiments have been carried out during this study to evaluate the performance of polymers in terms of adsorption and dynamic retention on sandstone core samples. The primary purpose was to investigate the applicability of acrylamide-based polymers in high salinity solutions. Brine water from the Uzen oil field with a concentration of 77,000 ppm was used to prepare polymer solutions. Moreover, the Uzen field conditions were recreated on a laboratory scale for coreflooding experiments. Thus, the temperature of 60^0 C was adjusted in a coreflooding system, and the concentrations of polymer solutions were set to achieve a target viscosity of 4 cp. The second and equally important aim of the study was to determine the optimum polymer concentration giving minimum adsorption. Rheological investigations that have been conducted previously were combined with static and dynamic adsorption tests. Thus, it was proposed to test the adsorption of polymers, which were investigated on different screening parameters such as concentration, thermal, mechanical and long-term stability that also considered the Uzen field conditions.

The concentrations of polymer solutions were observed by quantitative determination of the absorption of analytes (polymer molecules) in the ultraviolet-visible spectral region via UV-vis Spectrophotometer. Several solutions with concentrations ranging from 100 to 2000 ppm have been prepared for each polymer to build a UV calibration curve. The calibration curve is used to identify the actual concentration of polymer molecules in the solutions after contact with sandstone cores.

In a static adsorption test, the Berea sandstone cores were crushed and mixed with polymer solutions on rollers. For dynamic adsorption tests, the same Berea cores with a diameter of 1.5 inches and a length of 3 inches were flooded with polymer at different flowrates varying from 0.5 cc/min to 5 cc/min. The following steps were suggested to evaluate proposed polymers according to static and dynamic adsorption:

- investigate the effect of time and liquid-solid ratio on static adsorption;
- flooding of proposed polymers with different concentrations into the core with no presence of oil (injectivity test);
- consider the effect of polymer concentration on adsorption for both static and dynamic tests;
- examine the effect of oil presence (oil displacement test) on dynamic adsorption level.

The paragraphs below give more details about the materials used and the procedures applied.

2.1 Materials

The materials used in this study, such as Uzen field brine, HPAM-based polymers, and sandstone outcrop core samples, are described in this section.

2.1.1 Core Samples

Since the Uzen reservoir is terrigenous, the Berea sandstone core samples were used for the experiments. Figure 21 shows the sample itself and its crushed powder form. The sandstone core was crushed to a size of 50 nm and washed out to get rid of the clay particles. A total of four core samples were used for dynamic tests and one for the static test. Routine Core Analysis (RCAL) was performed on all samples before they were used in the experiments.

Figure 21. Core sample and sand powder used for adsorption tests

2.1.2 Brine

De-ionized (DI) water was used to synthesize formation water of the Uzen field which was used as a brine base for polymer solutions (Research and Design center “Nedra” LPP). The ion composition of water is 77000 ppm in total as shown in Table 9, Table 10 presents the mass of salts required to prepare the brine.

Table 9. Chemical composition of Uzen brine

Ions	Concentration for Uzen brine, ppm
Na^{+}	23426
Ca^{+2}	4448
Mg^{+2}	1300
Cl^{-}	46731

Table 10. Mass of salts required to prepare the brine

Salts	Mass for brine, g/L
NaCl	59.55
$CaCl_2*2H_2O$	12.32
$MgCl_2*6H_2O$	10.86

2.1.3 Polymers

Three HPAM-based polymers Superpusher SAV 10, SAV 19, and SAV 10 XV in powdered form were used in this work. The polymers were provided by SNF Floerger Company. Superpusher SAV series are the co-polymers or ter-polymers with functional groups of Acrylamide (AM), Acrylamido-Tert-Butyl-Sulfonate (ATBS) and N-Vinyl-Pyrrolidone (NVP) (Quadri et al., 2015). These types of polymers are known to be among the most stable polymers at high temperatures and high salinity. Figure 22 shows the chemical structure of HPAM-based SAV polymers.

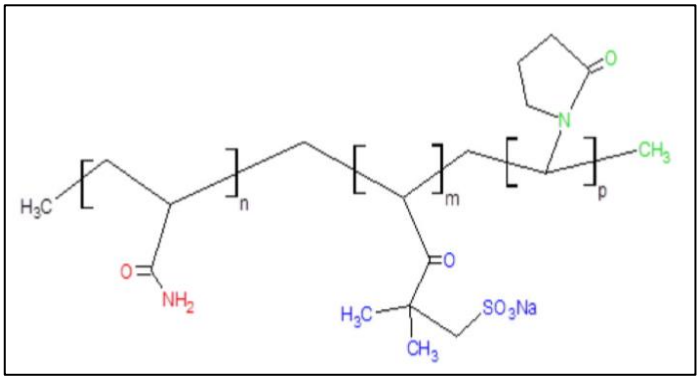

Figure 22. Ter-polymer of acrylamide, ATBS and NVP

2.2 Procedure

2.2.1 XRD Analysis for Berea sandstone

XRD for Berea Sandstone

Since the objective of the work is related to the Uzen field, which consists of sandstone reservoir rock, Berea sandstone outcrop core samples were used as porous media. The crushed sandstone core sample was analyzed using X-Ray Diffraction (XRD) apparatus to investigate the mineralogical composition of the Berea sandstone. Figure 23 presents the X-ray Diffraction (XRD) System by SmartLab (Rigaku). According to Table 11, the XRD analysis of the crushed rock sample shows that the rock predominantly consists of quartz (87.7%), K-feldspar (8.4%), kaolinite (2.5%), albite (1.1%) and only trace amounts of reactive clay species.

Figure 23. X-ray Diffraction (XRD) System by SmartLab (Rigaku)

Table 11. Mineral composition of Berea sandstone by XRD analysis

Mineral	**Composition (%)**
Quartz	87.7
K-feldspar	8.4
Kaolinite	2.5
Albite	1.1
Illite/Muscovite	0.3
Smectite	Trace
Calcite	Trace

2.2.2 Sand preparation

The sandstone cores were crushed using a disk chipper with a fixed distance between the disks of 50 nm. The disk chipper that was used illustrated in Figure 24. The resulting powder was washed in stages with de-ionized water to clean up the clay particles. After that, sandstone powder was soaked in hexane for a duration of 4 hours to get rid of any residual impurities followed by drying at 80°C for 24 hours (Li et al., 2017).

Figure 24. Disk chipper Retsch DM200 for crushing sandstone chunks

2.2.3 Core preparation

4 core samples were prepared to conduct three injectivity tests and an oil displacement test. Primarily, each core sample was dried in the oven for 12 hours at 80 ºC. Drying completed when the core samples reach a stable weight, which means that all water has been removed from pore space. After measuring the dry weight of samples, their porosity was defined using a Vinci Helium Porosimeter which is presented in Figure 25.

Figure 25. Vinci Helium Porosimeter

The core samples were then saturated with formation water of Uzen field, using Vinci Manual Saturator (AP-007-001-1), which is illustrated in Figure 26. Then porosities of core samples were calculated by using saturated core weight, dry core weight, formation water density and a bulk volume of core sample as demonstrated in Equation below. The samples were evacuated by a vacuum pump for 1 hour, then the saturation pressure was set to 1000 psi pressure for 4-6 hours until the stable pressure.

$$\emptyset_{wt} = \frac{V_b - \left(\frac{w_{wet} - w_{dry}}{\rho_w}\right)}{V_b}$$

Absolute permeability by brine and effective oil permeability for each sample were measured by the Vinci Aging cell apparatus. Darcy's law was used for intermediate calculations of permeability by integrating the pressure drop, flow rate, fluid viscosity and core dimensions using equiation:

$$k = \frac{q\mu L}{A\Delta p}$$

Figure 26. Vinci Manual Saturator (AP-007-001-1)

The absolute and effective permeability values for all core samples are presented in Table 12.

Table 12. Core samples properties

Sample #	Diameter, cm	Length, cm	Dry weight, g	Pore Volume, ml	Porosity, %	Absolute permeability, mD
Core #1 (SAV 10 injection)	3.80	7.69	183.00	16.95	0.193	56.98
Core #2 (SAV 19 injection)	3.81	7.66	184.42	17.14	0.196	82.86
Core #3 (SAV 10 XV injection)	3.80	8.00	193.13	17.78	0.196	21.76
Core #4 (SAV 10 oil dispacement)	3.80	7.69	181.13	17.58	0.20	90.27

2.2.4 Brine and polymer preparation

The required amount of different salts, such as NaCl, $CaCl_2*2H_2O$, and $MgCl_2*6H_2O$, were added into the DI water and mixed to obtain the formation water of the Uzen oilfield. The process of mixing was carried out using magnetic stirrers at 800 rpm for 1 hour to get a clear solution without precipitated salts. The resulting saline solution was used as a brine base for preparing all 3 polymer solutions.

The polymer solutions were prepared according to API Recommendation 63 (API RP 63, 1990). The bottom of the water vortex should expand 75% into the solution while using a magnetically driven stirrer. To get proper wetting, the dry polymer should be sprinkled evenly just below the top curve or shoulder of the vortex for 30 seconds. In case of rapid adding of polymer, the bunches of a non-hydrated polymer may occur, which is called “fish-eye”. After adding the polymer powder into the brine, the solution should be stirred at 80-100 rpm for 3 hours to keep the solid particles from settling at the bottom of the beaker. The higher rotation rates may cause the breaking of polymer chains which leads to viscosity loss. The proper procedure of mixing polymer solutions is illustrated in Figure 27.

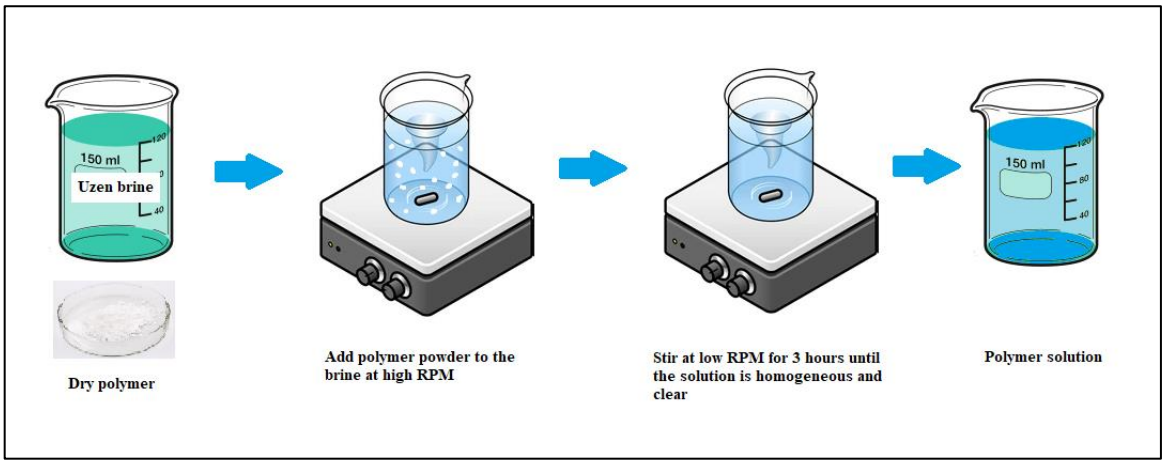

Figure 27. Polymer preparation process

2.2.5 UV Calibration Curve

The UV calibration curve is the key technology for identifying the actual concentrations of polymer solutions before and after adsorption experiments. The calibration curve for a certain polymer provides the linear dependence of UV absorbance to the mass concentration of the polymer, which allows identifying the actual concentration of effluents knowing only absorbance value. Four or more concentrations for each polymer solution were prepared initially to obtain the values of UV absorbance analysis. In order to construct the most accurate curve, the range of concentrations tested should include those concentrations used in adsorption experiments. Samples were taken in a volume of 1-1.5 ml and tested on UV Spectrophotometer using quartz sample cuvettes. The use of cuvettes made of quartz was crucial, as conventional plastic cuvettes lead to large interferences on the polymer absorbance values. Figures 28, 29 demonstrate the UV device and sample cuvettes used in this study.

Figure 28. Evolution 300 UV-vis Spectrophotometer

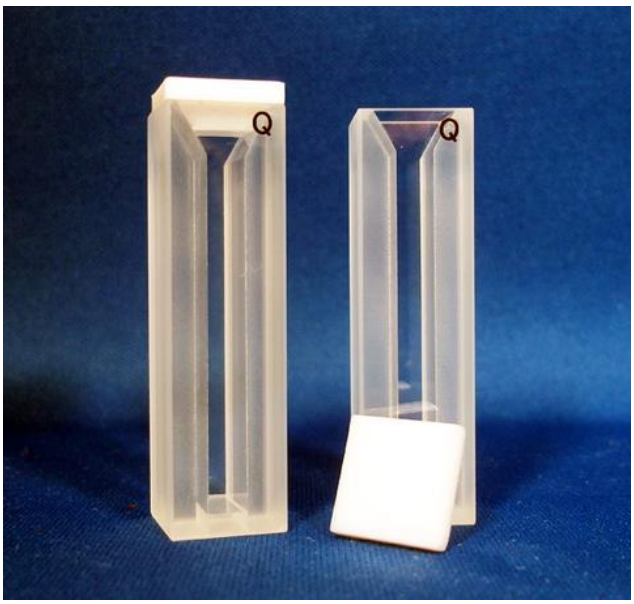

Figure 29. Quartz cuvettes used for UV tests

Another thing to mention, before all samples are tested the brine water which was used for polymer solutions should be run through the UV device as a baseline. The considering of baseline water at the beginning promotes obtaining the UV absorbance values for polymers only. The absorbance values of the salts in the brine are subtracted automatically and ignored during UV testing of polymers.

2.2.6 Static Adsorption Test

The main idea for evaluating the adsorption level is to identify the difference in polymer concentration before and after adsorption by using the obtained calibration curve. After finding the concentration difference, the adsorption level is calculated based on the following equation (Li et al., 2017):

$$q_{static} = \frac{V(C_0 - C_e)}{G}$$

where q is the adsorption level (μg/g); V is the volume of polymer (L); C_0 is the initial concentration of polymer in the solution (ppm); C_e is the concentration of effluent after the mixing (ppm); G is the weight of used sand (g).

It was decided to investigate the static adsorption of the SAV 10 polymer as it showed the best performance in rheological and degradation experiments conducted by my colleague (Bekpayev, 2021). The effect of different aspects, such as time, concentration, and liquid-solid ratio have been observed during the static test. Three polymer concentrations: 800 ppm, 1000 ppm, and 1200 ppm were considered in this experiment. It is crucial to mix substances applying

only external forces out of the tank, because using stirrers may cause the polymer chains breakage. Therefore, it was concluded to use ageing cells to keep mixtures sealed as shown in Figure 30. And a roller oven provided by OFI Testing Equipment, which is illustrated in Figure 31 is used for the proper mixing of polymers and sand. 250 ml of the polymer solutions have been weighed, and according to values, the weights of sand were calculated considering liquid-solid ratios of 2:1 and 5:1.

Figure 30. Ageing cells used for mixing in static adsorption test

Figure 31. OFITE roller oven used in the static adsorption test

The mixtures of polymer and sand were put on rotating rollers for 48 hours. They were sampled for every 2 hours in the duration of the first 10 hours. After all the samples were collected, they were left for 24 hours to allow the fine mechanical particles to precipitate out. Clean effluents

were taken from the top of the mixture and tested on UV-vis Spectrophotometer. A total of 35 samples were tested for the static adsorption test.

2.2.7 Injectivity and Oil Displacement Test

Coreflooding designs for injectivity and oil displacement test were taken from analogue research conducted by Quadri et al. (2015). Thus, waterflooding was conducted before and after polymer injection as a pre and post-flush. A more detailed coreflooding design according to Quadri et al. (2015) is illustrated in Figure 32.

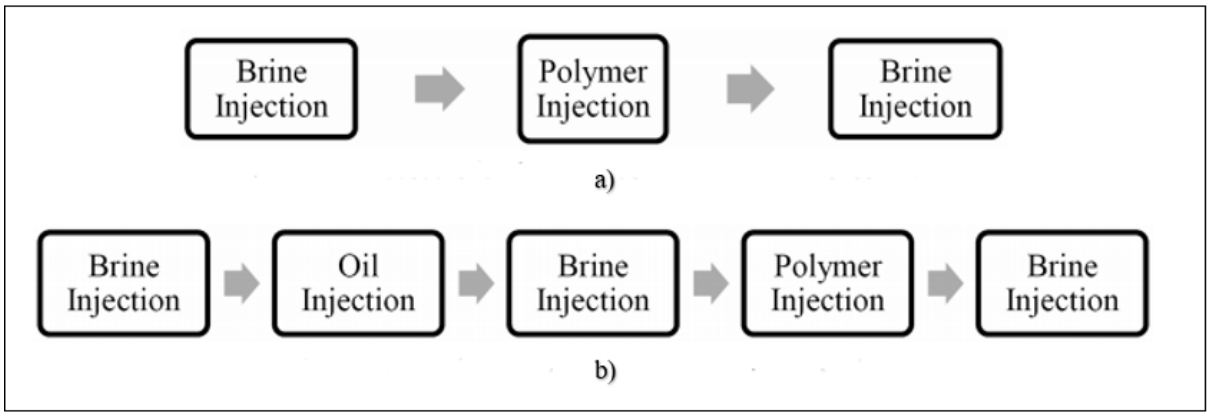

Figure 32. a) procedure for the dynamic adsorption in the absence of oil b) procedure for the dynamic adsorption in the presence of oil

Dynamic adsorption of proposed polymers was tested during the injectivity experiments. 9 polymer coreflooding tests were conducted in water-wet cores and 1 dynamic adsorption test was done during the oil displacement experiment. The coreflooding experiments were conducted with the confining pressure of 1000 psi and the temperature of 60 ºC using the aging cell apparatus which is shown in Figure 33. Table 13 provides detailed information about core flooding experiments design. For each polymer flooding experiment, the effluent samples were taken every 2-3 mL till 1 PV reached, after that samples were taken from each PV. The reason for gaining the effluent sample every 2-3 mL is to monitor the transition between pre-flush brine effluent and polymer effluent. Thus, from each experiment, 75-84 samples of polymer effluent were tested through the UV-Spectrophotometer, resulting in a total of 260 effluent samples.

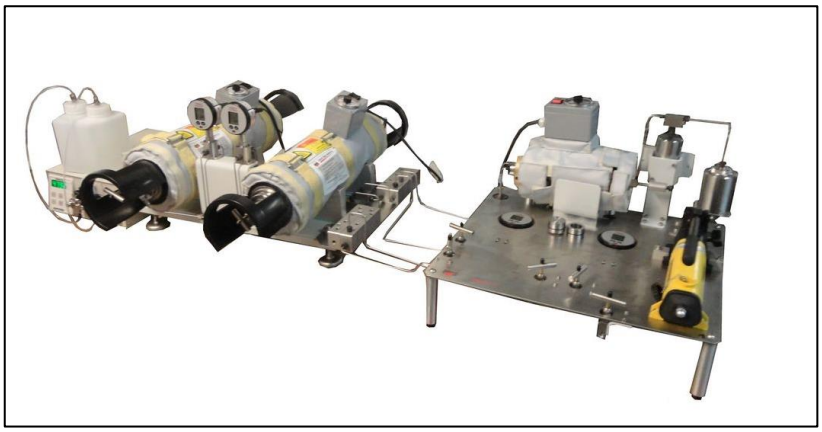

Figure 33. Aging cell apparatus (Vinci Technologies)

Table 13. Core flooding experiment designs

Core #	Experiment #	Injection sequence	Flow rates, cc/min
1	1	Pre-flush brine (Uzen FW)	0.5, 1, 1.5, 2, 5
		SAV 10 – 2500 ppm	
	2	SAV 10 – 1250 ppm	
	3	SAV 10 – 625 ppm	
		Post-flush brine (Uzen FW)	5
2	4	Pre-flush brine (Uzen FW)	0.5, 1, 1.5, 2, 5
		SAV 19 – 1800 ppm	
	5	SAV 19 – 900 ppm	
	6	SAV 19 – 450 ppm	
		Post-flush brine (Uzen FW)	5
3	7	Pre-flush brine (Uzen FW)	0.5, 1, 1.5, 2, 5
		SAV 10 XV – 1000 ppm	0.5, 1, 1.5, 2
	8	SAV 10 XV – 500 ppm	0.5, 1, 1.5, 2, 5
	9	SAV 10 XV – 250 ppm	
		Post-flush brine (Uzen FW)	5
4	10	Pre-flush brine (Uzen FW)	0.5, 1, 1.5, 2, 5
		Oil	
		Brine	
		SAV 10 – 2500 ppm	
		Post-flush brine (Uzen FW)	5

2.2.8 Dynamic Adsorption Test

An important aim of the dynamic adsorption test was to properly sample the effluent coming out of the sandstone core. The procedure of determining actual concentration after adsorption was the same as in the static test. After samples were tested on UV Spectrophotometer, the calculation of dynamic adsorption were conducted as follows (Ahmadi et al., 2015):

$$q_{dynamic} = \frac{C_0 V_0 - \sum_{i=1}^{n} C_e V_e}{W}$$

where C_0 and V_0 represent initial solution concentration (ppm) and total injected volume (mL) respectively; C_e and V_e stand for effluent concentration (ppm) and the volume of taken sample (mL); W is the dry weight of sandstone core.

The adsorption levels were obtained by measuring the concentration of effluent samples via UV-vis Spectrophotometer. The flowrates of 0.5 cc/min, 1 cc/min, 1.5 cc/min, 2 cc/min, 5 cc/min were applied. The polymers SAV 19, SAV 10, SAV 10 XV were injected with the concentration of 1800 ppm, 2500 ppm, and 1000 ppm respectively. Since the injectivity test was carried out in parallel, the polymer concentrations were reduced by a factor of 2 and 4 during the coreflooding.

3 RESULTS

This chapter presents and discusses the obtained results of experiments described in the methodology section. Laboratory studies were designed to estimate the adsorption properties of three polymers. Before the experiments, calibration curves for each polymer were built by quantifying polymer molecules in virgin solutions. The effect of mixing time, liquid-solid ratio, and concentrations were examined during the static adsorption experiment.

Investigations of the concentration effect on the dynamic retention were carried out during the injectivity tests. As a result, three used polymers were evaluated in terms of dynamic adsorption. SAV 19 polymer resulted in the lowest dynamic adsorption, and SAV 10 XV demonstrated a quite similar result. As previously mentioned, the SAV 10 polymer was selected for its rheological properties. Further, this polymer was flooded into the core with the presence of oil to examine the effect of the oil on adsorption.

3.1 UV Calibration Curve

Three polymer solutions with different concentrations were tested on the UV Spectrophotometer. Figures 34, 35, 36 demonstrates the value of absorbed xenon rays into molecules of SAV 10, SAV 19, and SAV 10 XV respectively.

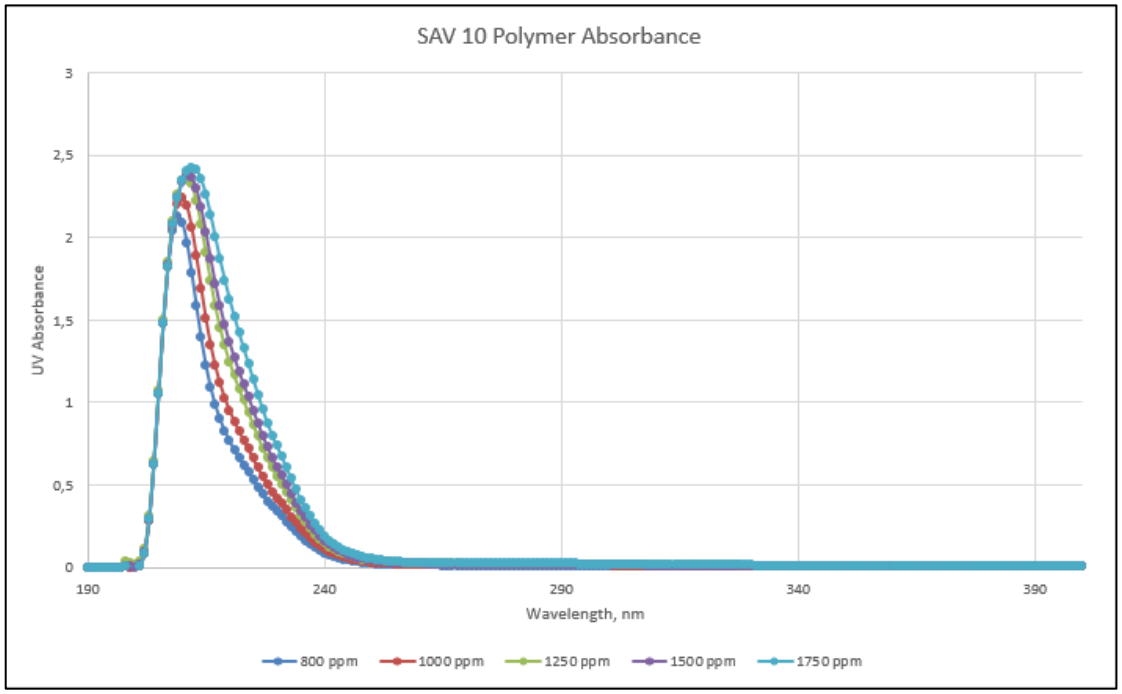

Figure 34. SAV 10 polymer operating absorbance spectral range

The maximum wavelength range of the used UV-vis Spectrophotometer was 190-1100 nm. However, the spectral range of 190-400 nm was used to speed up the UV process. Moreover, the tested SAV 10 polymer operated in the range of 205-215 nm as shown in the graphs.

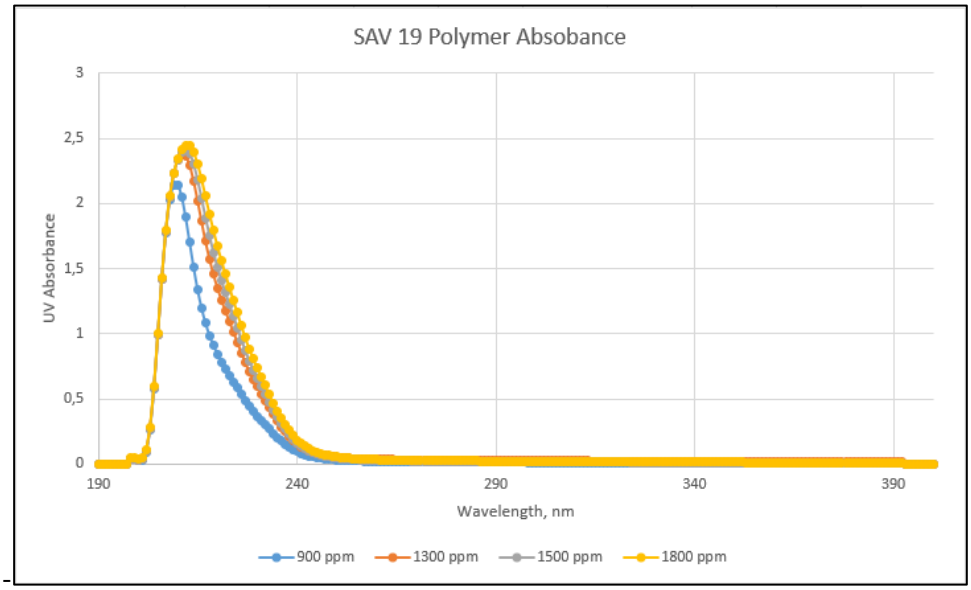

Figure 35. SAV 19 polymer operating absorbance spectral range

The SAV 19 polymer has resulted in a narrower range of 208-214 nm, which can be caused by the lightest molecular weight of the polymer among others. According to SAV 10 XV, it can be seen that the shape of the curves differentiates from the other two polymers. Also, the molecular weight of the polymer should be considered to explain this behaviour. As the molecular weight of SAV 10 XV is the highest one, the obtained spectral range of this polymer is 209-221 nm.

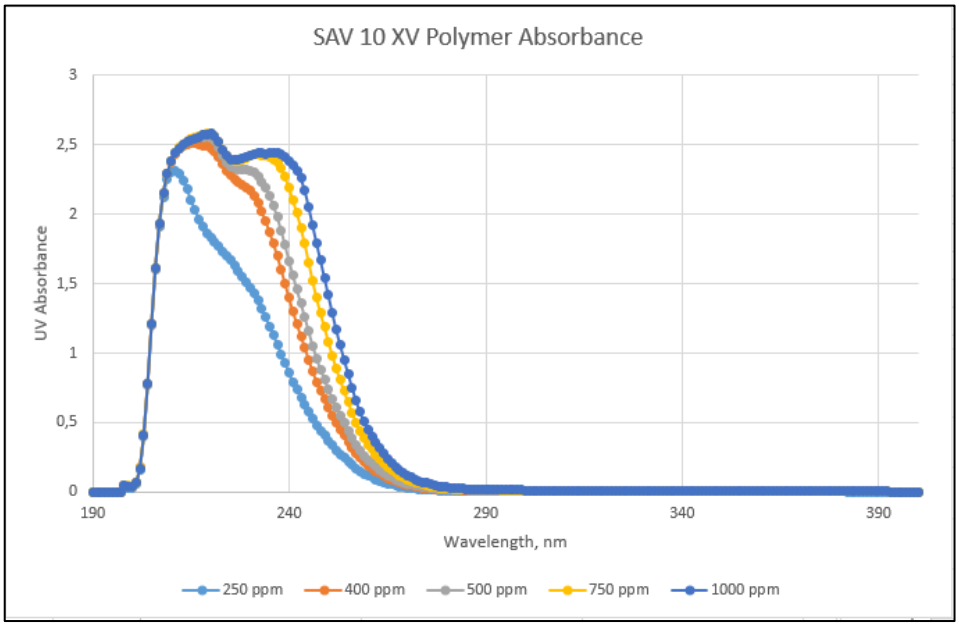

Figure 36. SAV 10 XV polymer operating absorbance spectral range

The peaks of each concentration were plotted on the Absorbance vs Concentration graph to construct calibration curves for each polymer type. The linear absorption dependence (equation straight-line) was obtained by applying a best-fit line for points. In fact, the dependence equations resulted with *y*-intersect term *b*, as shown in Table 14, where *y* stands for absorbance and *x* for concentration. Three calibration curves were established as shown in Figures 37, 38, 39.

Table 14. Linear absorbance dependence on mass concentration of SAV 10, SAV 19, SAV 10 XV

Polymer type	**Equation of straight-line**
SAV 10	y = 0.0003x + 1.9741
SAV 19	y = 0.0003x + 2.049
SAV 10 XV	y = 0.0003x + 2.514

Theoretically, zero concentration of polymer in the solution should give zero absorbance and accordingly, the *b* term should not exist. Therefore, *b* term values were subtracted from absorbance to correct the line to the origin. Thus, the calibration curves for polymers SAV 10, SAV 19, and SAV 10 XV were obtained as shown in Figures 37, 38, 39.

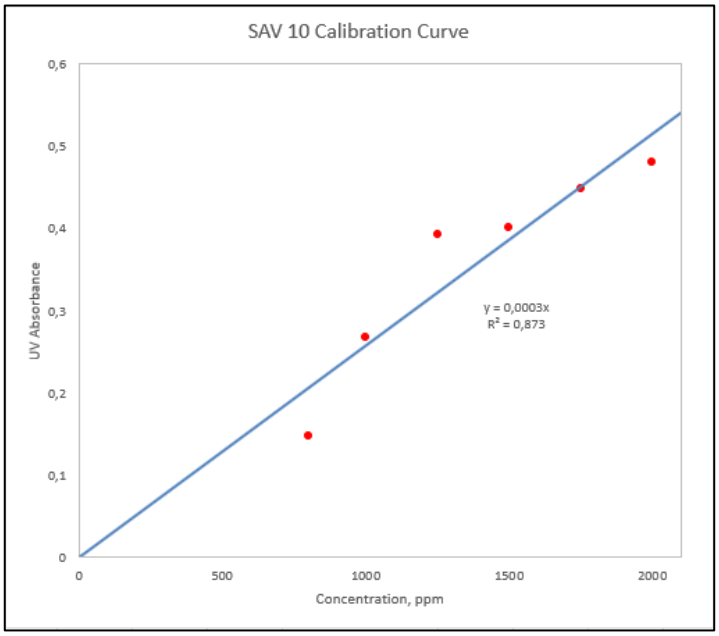

Figure 37. UV calibration curve for SAV 10 polymer

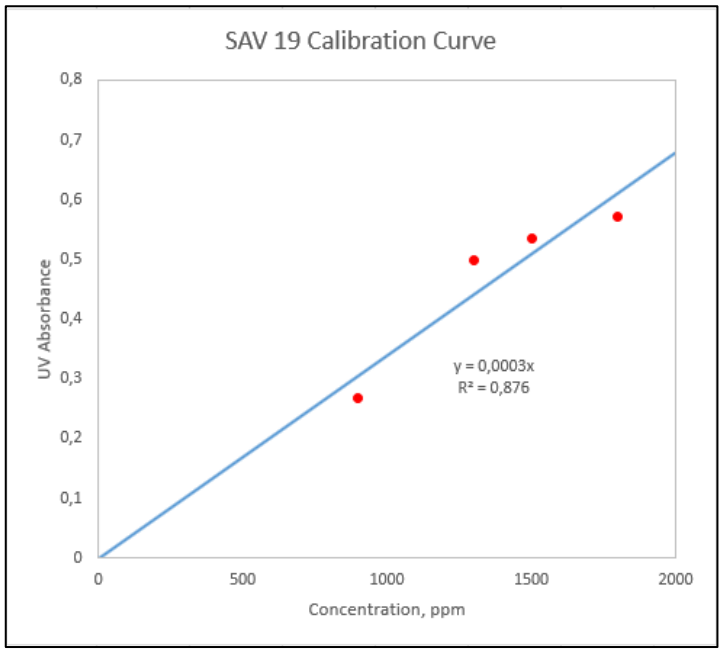

Figure 38. UV calibration curve for SAV 19 polymer

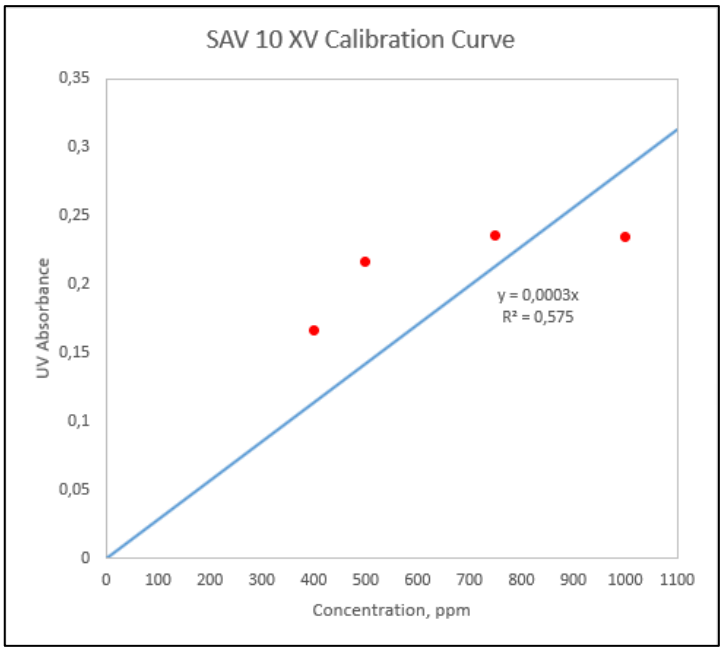

Figure 39. UV calibration curve for SAV 10 XV polymer

The UV calibration curve for the SAV 10 XV may not appear to follow a linear trend as shown in Figure 39. Nevertheless, it was decided to apply a linear equation for the points due to several reasons. The linear behaviour can be noticed within a certain range, but out of this range, it reaches a plateau where all values are almost the same. This is the limitation of the UV Spectrophotometry tool. The only solution to this issue can be a dilution of the used polymer solution. In that case, the dilution factor must be considered for all tested effluents which quantity was about 300 for experiments. However, the dilution and mixing of 2 ml effluents are

inappropriate in terms of time. Therefore, the linear equation was applied by averaging all obtained absorbance values.

3.2 Static Adsorption

3.2.1 Liquid-Solid Ratio Effect

The effect of the liquid-solid ratio was investigated by conducting two static tests considering the ratio of 2:1 and 5:1. It was noticed that the adsorption level increases with an increasing ratio. Figure 40 illustrates the difference between applying two liquid-solid ratios during the static test. Li et al., (2017) were the first scientists who implemented an approach to the effect of liquid-solid ratio on polymer adsorption. According to the authors, the magnitude of KYPAM polymer adsorption almost leveled off beyond the ratio of 30:1 in the Adsorption vs LSR plot. Therefore, it can be assumed that SAV 10 polymer could follow the same scenario since KYPAM is also polyacrylamide-based.

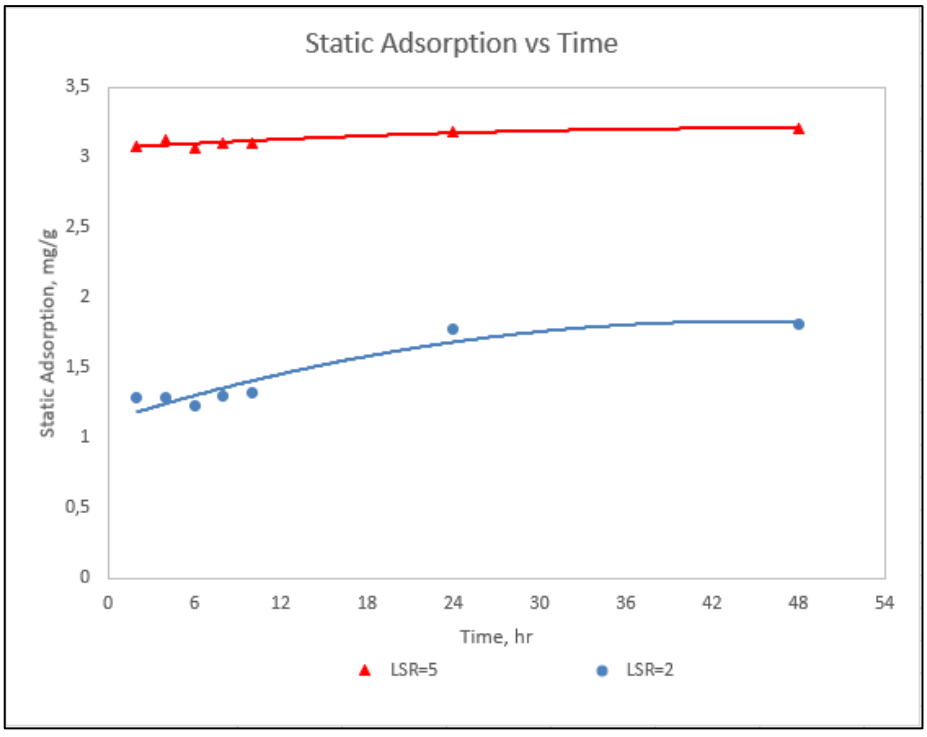

Figure 40. The effect of liquid-solid ratio on static adsorption (SAV 10, 1000 ppm)

3.2.2 Time and Concentration Effect

The impact of mixing time on static adsorption can also be seen in the graph above. It is clearly shown that the level of static adsorption increases with soaking time. Solutions were sampled in stages over the first 10 hours according to the lab access limit. Accordingly, the values of this section are rising smoothly until the equilibrium adsorption state has been reached between

24 and 48 hours. Such a behaviour of the adsorption magnitude can be explained by the required time for HPAM-based polymers to reach an equilibrium state. Usually, the HPAM-based polymers require more time due to their macromolecular long-chain structure. Moreover, the process of polymer conformation increases the amount of molecules that have been stuck on the surface. The presence of loops and tails of adsorbed polymer molecules is a favourable condition for the bonding of the remaining free molecules.

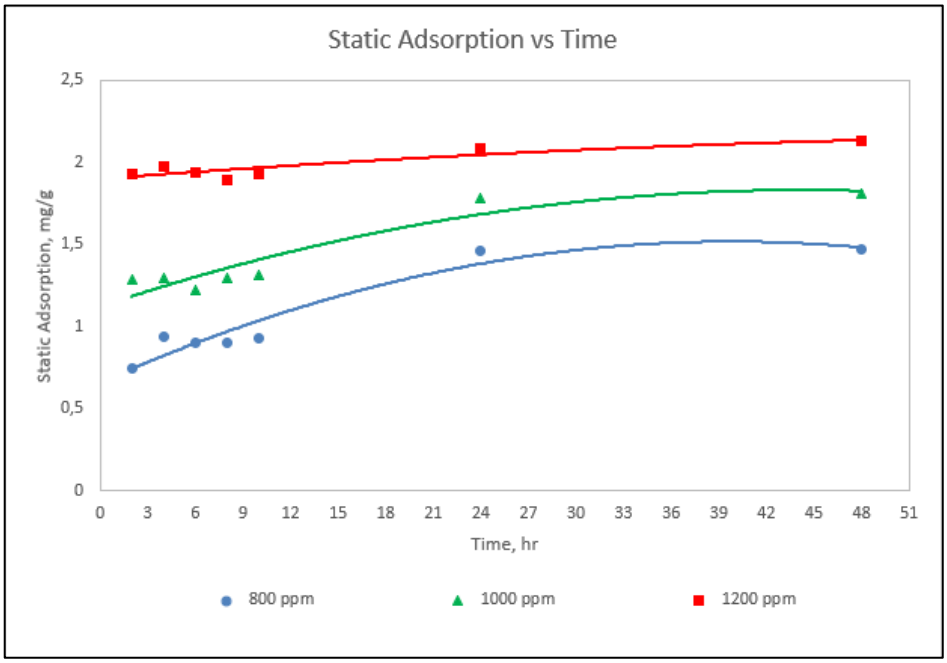

Figure 41. Static adsorption test with LSR=2 for SAV 10 polymer

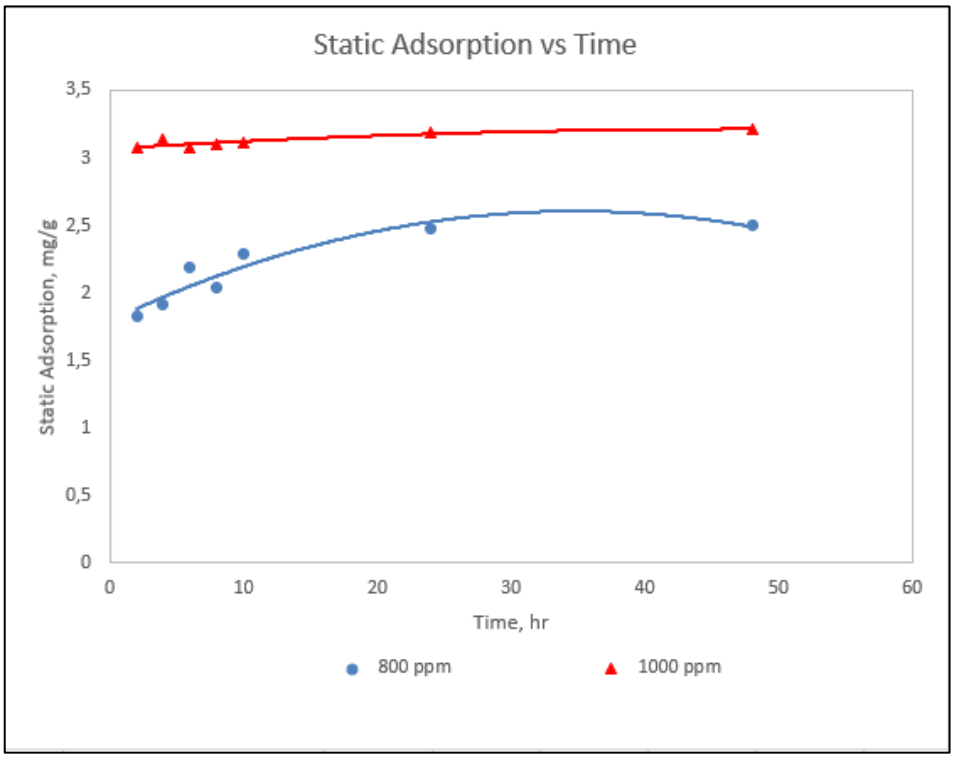

Figure 42. Static adsorption test with LSR=5 for SAV 10 polymer

The effect of concentration has also been carried out during this test. It was observed that adsorption level is increased with concentration as shown in Figures 41, 42. Besides, the higher the concentration, the adsorption magnitude becomes more flattened. This behaviour can be attributed to a fact that the high presence of polymer molecules motivates a more progressive adsorption process to occur. Thus, the adsorption equilibrium state is reached faster in high mass concentrations. Different concentrations were applied in both static tests according to two liquid-solid ratios. The values of adsorption for each concentration and mixing time are presented in Table 15.

Table 15. Static adsorption values depending on time and concentration

800 ppm (LSR=2)							
Time, hr	2	4	6	8	10	24	48
Concentration difference, ppm	200.33	253.67	243.67	243.67	250.33	393.67	396.90
Static Adsorption, mg/g	0.74	0.94	0.90	0.90	0.93	1.46	1.47
1000 ppm (LSR=2)							
Time, hr	2	4	6	8	10	24	48
Concentration difference, ppm	347.72	348.97	331.16	351.16	356.16	480.53	488.70
Static Adsorption, mg/g	1.29	1.29	1.23	1.30	1.32	1.78	1.81
1200 ppm (LSR=2)							
Time, hr	2	4	6	8	10	24	48
Concentration difference, ppm	522.09	533.97	523.03	512.41	522.41	563.97	575.10
Static Adsorption, mg/g	1.93	1.98	1.94	1.90	1.93	2.09	2.13
800 ppm (LSR=5)							
Time, hr	2	4	6	8	10	24	48
Concentration difference, ppm	197.00	207.00	237.00	220.33	247.00	267.00	270.00
Static Adsorption, mg/g	1.82	1.92	2.19	2.04	2.29	2.47	2.50
1000 ppm (LSR=5)							
Time, hr	2	4	6	8	10	24	48
Concentration difference, ppm	332.41	338.34	331.78	335.22	335.84	344.59	346.68
Static Adsorption, mg/g	3.08	3.13	3.07	3.10	3.11	3.19	3.21

3.3 Dynamic Adsorption

3.3.1 Effect of flowrate

Five different flowrates were applied, the sequence of which is from low to high during the injectivity test. However, the maximum flowrate of 5 cc/min was excepted for 1000 ppm SAV

10 XV polymer because of pressure overload of coreflooding system caused by high molecular weight. Thus, the effluent samples during every injection flowrate were collected excluding 1000 ppm of SAV 10 XV. No effect of flowrate on dynamic adsorption was investigated since the difference between initial and effluent concentration holds almost constant as shown in Figures 43, 44, 45.

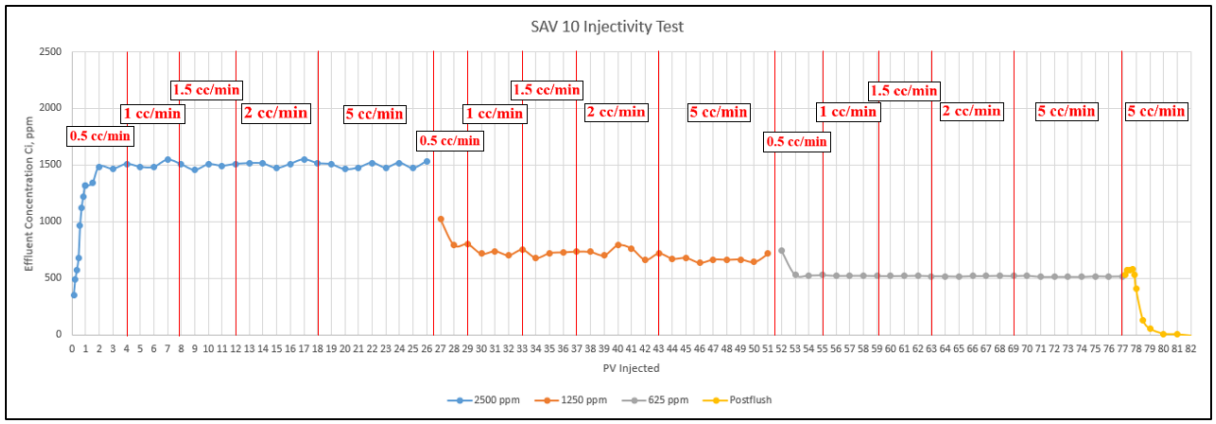

Figure 43. SAV 10 effluent concentrations obtained during the injectivity test

All effluent samples of SAV 10 polymer were tested on the UV device. A plateau of effluent concentrations was noticed despite changes in injection rates. The type of retention which can be caused by varying injection rates is hydrodynamic retention, which is not explained properly yet (Chauveteau and Kohler, 1974). However, as Sorbie (1991) provides, this type of retention has not a big contribution to the overall retained polymer amount. Therefore, it can be stated that the dynamic adsorption level does not change with flowrate.

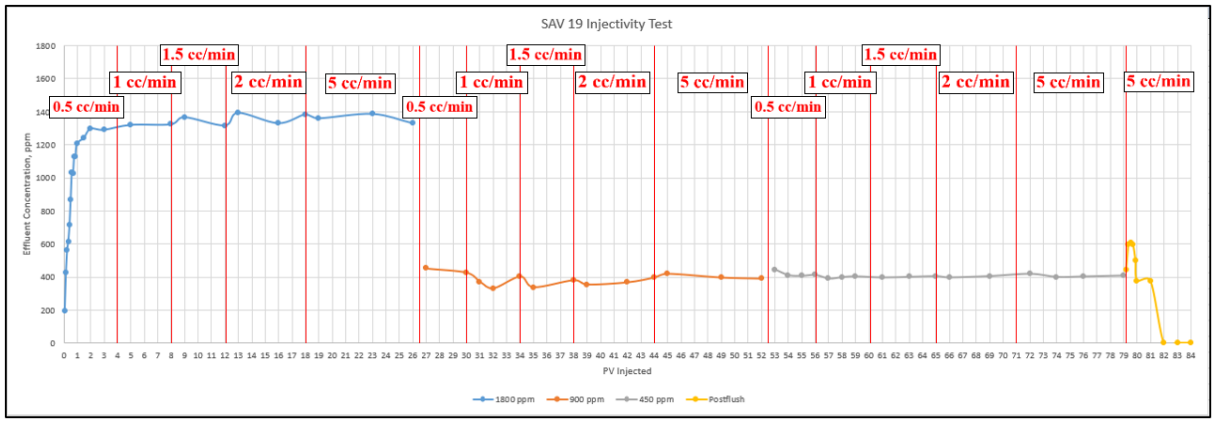

Figure 44. SAV 19 effluent concentrations obtained during the injectivity test

Also, it was noticed that the effluent concentrations are more stable at the injection of initially lower concentrations such as 625 ppm for SAV 10, 450 ppm for SAV 19, and 250 ppm for SAV 10 XV. However, in the next stage (post-flushing) it was shown that the concentration

magnitude jumped sharply. This could be caused by the breakthrough of bonded polymer chains that were occurred during the polymer flooding. The same behaviour was also noticed for post-flushing after injection of SAV 10 XV.

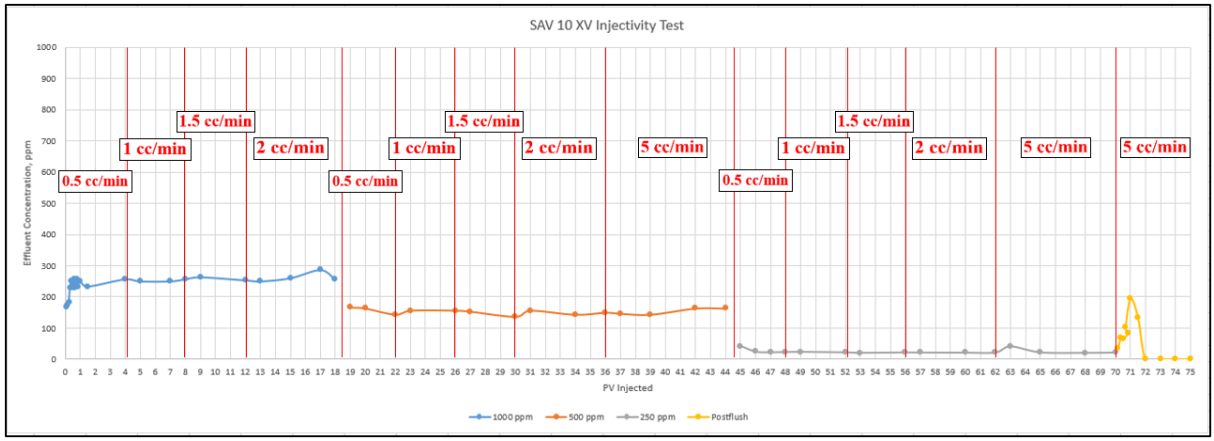

Figure 45. SAV 10 XV effluent concentrations obtained during the injectivity test

3.3.2 Effect of concentration

Based on the statement that flowrates have no effect, it was decided to calculate the dynamic adsorption within the first flowrate of 0.5 cc/min. Also, the calculation was conducted considering only stabilized values of concentrations after the first injected pore volume until the flowrate change. Moreover, it can be supported by the fact that the adsorption phenomena mainly occurs in the first stages of coreflooding or near-wellbore during field tests (Sheng, 2011). Obtained values of dynamic retention for used polymers are presented in Figures 46, 47, 48. The maximum concentrations of polymers were selected as 2500 ppm for SAV 10, 1800 ppm for SAV 19, and 1000 ppm for SAV 10 XV according to the rheological experiments considering a target viscosity of 4 cp which was carried out before the adsorption tests. The high sensitivity of polymer adsorption to mass concentration was established as a result of the dynamic test.

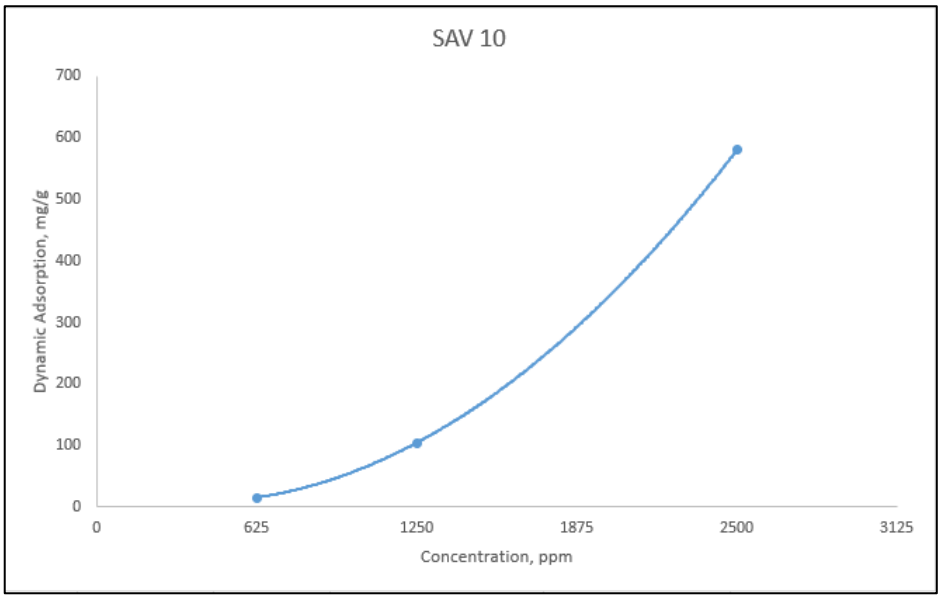

Figure 46. Dynamic adsorption of SAV 10 polymer for different concentrations

The dynamic adsorption of SAV 10 polymer showed the highest result of 580.03 µg/g among the other two polymers. Accordingly, the worst performance in terms of adsorption properties was observed by SAV 10 despite all its rheological and stability priveledges. Obtained dynamic adsorption curve shows the drastic increase with polymer concentration. Moreover, the used concentration of 2500 ppm was the highest in comparison with SAV 19 and SAV 10 XV concentrations. Based on these facts, the high adsorption level of SAV 10 polymer is the reasonably expected result. However, the promising injectivity results of SAV 10 which were observed by my colleague prompted the oil displacement test to conduct.

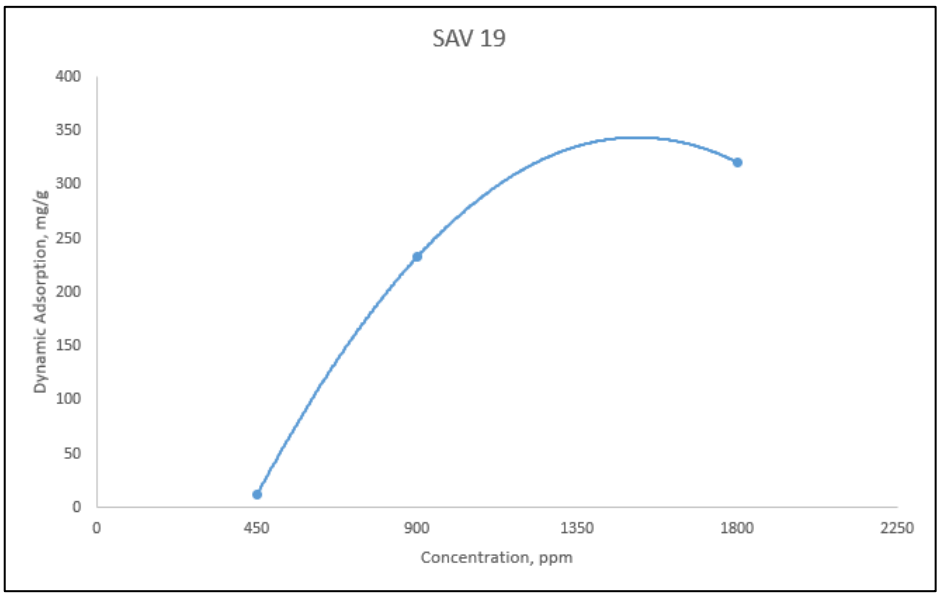

Figure 47. Dynamic adsorption of SAV 19 polymer for different concentrations

SAV 19 polymer adsorption was the lowest one for the dynamic test resulting in the value of 320.97 µg/g. Since the difference between adsorption levels for 900 ppm and 1800 ppm injections is not so great, the declining adsorption trend can be observed on the graph. Therefore, this polymer could be the most promising in terms of adsorption. If the choice of polymer for the Uzen field is reconsidered, SAV 19 polymer would be an appropriate choice due to its economic feasibility. The cost of the polymer project will be more favourable since it will require less polymer raw material. In other words, SAV 19 polymer has a relatively low molecular weight thereby less concentration should be prepared to achieve a target oil viscosity. However, it is important to mention that the injection procedure of SAV 19 requires higher pressures than it was for SAV 10, so it will call for more power treatment in field pilot tests.

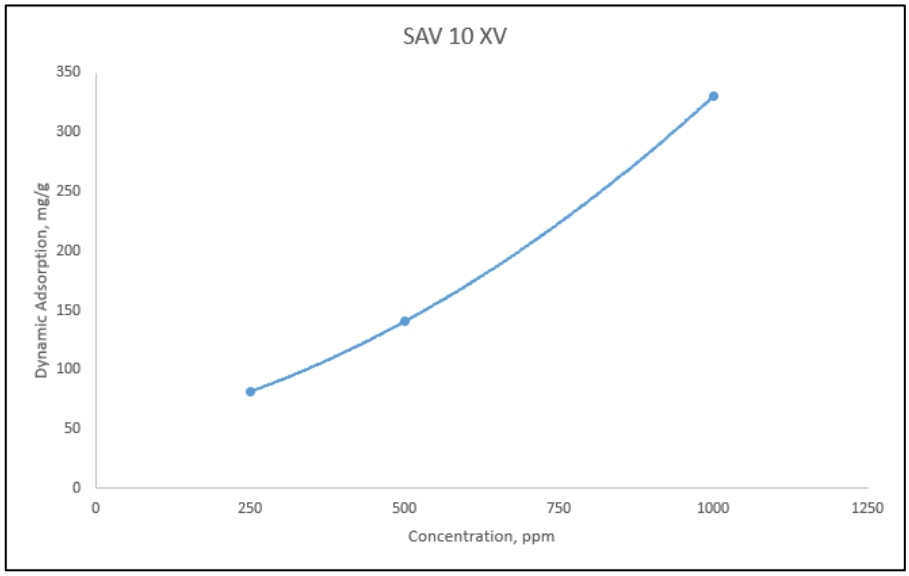

Figure 48. Dynamic adsorption of SAV 10 XV polymer for different concentrations

Regarding SAV 10 XV adsorption, it showed quite similar results to SAV 19 polymer. However, the high molecular weight of this polymer and unsatisfying results in mechanical and thermal degradation may lead to several difficulties such as high injection pressures, a significant mechanical entrapment in low permeable zones, and a huge loss of viscosity by time.

All obtained results for coreflooding tests were summarized in Table 16 including the oil displacement test.

Table 16. Dynamic adsorption values for acrylamide-based polymers

Polymer	Core PV, ml	Permeability, mD	Injected PV	Concentration, ppm	Dynamic Adsorption, mg/g
SAV 19	17.14	82.86	26	1800	320.97
			26	900	232.73
			27	450	11.53

SAV 10 XV	17.78	21.76	18	1000	330.28
			26	500	140.55
			26	250	81.56
SAV 10	16.95	56.98	26	2500	580.03
			25	1250	104.45
			26	625	15.43
SAV 10 (Oil presence)	17.58	74.74	15	2500	533.30

The dynamic adsorption test of SAV 10 polymer with oil presence showed less value than the test with no oil. Accordingly, the presence of oil in the core positively impacts dynamic adsorption. Nevertheless, the difference between the core permeabilities should be taken into account, as permeability is one of the most influential parameters. Also, the wettability of core samples is important to consider during the dynamic tests. Theoretically, water-wet cores provide a higher oil recovery due to low residual oil saturation. If the core sample is oil-wet, this affects less contact of the polymer and the rock surface and therefore less adsorption could take place. Besides, the lowering of the adsorption level of SAV 10 should be developed by considering chemical additives such as alkalis which improve the ion charge of polymers.

4 CONCLUSIONS AND RECOMMENDATIONS

In this study, the adsorption properties of acrylamide-based polymers have been investigated under the Uzen field conditions. The effect of liquid-solid ratio, mixing time, and concentration on static adsorption was examined. Dynamic adsorption test was carried out in parallel with the injectivity and oil displacement tests. As a result, the relation between adsorption and mass concentration was obtained. Also, the effect of the presence of oil in the core was observed. Based on the results, the following outcomes can be found:

- The high sensitivity of polymer adsorption to concentration was observed during static and dynamic tests. Static adsorption changes drastically with a change in concentration of only 200 ppm. Most likely static adsorption increases until the plateau value is reached.
- SAV 19 polymer adsorption was the lowest one for the dynamic test resulting in the value of 320.97 μg/g. Thus, SAV 19 can be assumed as a suitable polymer for the Uzen field conditions, but only from an adsorption point of view. The dynamic adsorption levels for SAV 10 XV and SAV 10 was obtained as 330.28 μg/g, and 580.03 μg/g, respectively.
- Despite the above results, the SAV 10 polymer remains in a privileged position due to its significant advantages in terms of rheological properties, mechanical, thermal, and long-term stabilities. In that case, the methods of lowering the SAV 10 adsorption should be taken into account and developed.
- Increasing the mixing time has a negative effect on static adsorption. However, the equilibrium adsorption state can be reached after 24 hours of mixing. Also, there is a possibility that the equilibrium state can be reached between 10 and 24 hours since there are missed data in this interval.
- Regarding the liquid-solid ratio effect, other values up to 30:1 should be applied for future static adsorption tests. According to the studies, the maximum adsorption value should be achieved by increasing the liquid-solid ratio.
- The minor effect of injection rates was noticed, therefore it can be neglected. According to this statement, it is recommended to inject a few pore volumes of the polymer at one fixed rate since it was enough to estimate the dynamic adsorption properties.
- The presence of oil in the core has a positive effect on dynamic retention with decreasing from 580.03 μg /g to 533.30 μg /g. However, the permeability for the oil displacement test was higher and the difference in permeability should be considered and evaluated.

Therefore, the use of homogeneous core samples is strongly recommended during laboratory experiments.

- In addition, the investigations on temperature effect, salinity effect, and adsorption on different minerals can be considered as recommendations for the further development of this project.

5 REFERENCES

Abidin, A.Z., Puspasari, T., Nugroho, W.A. 2012. Polymers for enhanced oil recovery technology, Procedia Chem. 4: 11–16.

Al-Abri, Sidiq & Amin, 2012. Mobility ratio, relative permeability and sweep efficiency of supercritical CO2 and methane injection to enhance natural gas and condensate recovery: Coreflooding experimentation. Journal of Natural Gas Science and Engineering, pp. 166-171.

Al-Hajri, Sameer & Mahmood, Syed & Abdulelah, Hesham & Akbari, Saeed. (2018). An Overview on Polymer Retention in Porous Media. Energies. 11. 10.3390/en11102751.

Ali, M. and Mahmud, H. B. 2015. The Effects of Concentration and Salinity on Polymer Adsorption Isotherm at Sandstone Rock Surface. IOP Conf Ser Mater Sci Eng 78: 012038, 7 pages. https://doi.org/10.1088/1757-899X/78/1/012038

API RP 63, Recommended Practices for Evaluation of Polymers Used in Enhanced Oil Recovery Operations. 1990. Washington, DC, USA: American Petroleum Institute

Argillier, J. F., Audibert, A., Lecourtier, J. et al. 1996. Solution and Adsorption Properties of Hydrophobically Associating Water-Soluble Polyacrylamides. Colloids Surf A Physicochem Eng Asp 113 (3): 247–257. https://doi.org/10.1016/0927-7757(96)03575-3

Bekpayev, I., 2021. Thesis – Application of Polymer Flooding in Sandstone Reservoirs of Uzen field. Nazarbayev University. 57-68

Brunauer, S., Deming, L. S., Deming, W. E. et al. 1940. On a Theory of the van der Waals Adsorption of Gases. J Am Chem Soc 62 (7): 1723–1732. https://doi.org/10.1021/ja01864a025

C & C Reservoirs. 2010. Former Soviet Union. Uzen Field South Mangyshlak Basin, Kazakhstan. Field Evaluation Report

Carraher, 2017. Introduction to Polymer Chemistry. 4 ed. Boca Raton: CRC Press.

Chauveteau, G., Kohler, N., 1974. Polymer flooding: The essential elements for laboratory evaluation. Presented at the SPE Improved Oil Recovery Symposium, Tulsa, 22–24 April.

Dang, T. Q. C., Chen, Z., Nguyen, T. B. N. et al. 2014. Investigation of Isotherm Polymer Adsorption in Porous Media. Pet Sci Technol 32 (13): 1626–1640. https://doi.org/10.1080/10916466.2010.547910

Deng, Y., Dixon, J. B., White, G. N. 2006. Adsorption of Polyacrylamide on Smectite, Illite, and Kaolinite. Soil Sci Soc Am J 70 (1): 297–304. https://doi.org/10.2136/sssaj2005.0200

Ferreira, V. H. S. and Moreno, R. B. Z. L. 2017. Impact of Flow Rate Variation in Dynamic Properties of a Terpolymer in Sandstone. J Pet Sci Eng 157: 737–746.

Firozjaii, A. M., Saghafi, H. R. 2019. Review on chemical enhanced oil recovery using polymer flooding: Fundamentals, experimental and numerical simulation. IOR/EOR Research Institute, National Iranian Oil Company, Tehran, Iran

Gramain, P. and Myard, P. 1981. Adsorption Studies of Polyacrylamides in Porous Media. J Colloid Interface Sci 84 (1): 114–126.

Hirasaki, G.J., and G.A. Pope. "Analysis of Factors Influencing Mobility and Adsorption in the Flow of Polymer Solution Through Porous Media." SPE J. 14 (1974): 337–346. doi: https://doi.org/10.2118/4026-PA

Hollander, Agnes, F., P. Somasundaran, Carl, C. 1981. Adsorption characteristics of polyacrylamide and sulfonate-containing polyacrylamide copolymers on sodium kaolinite. *Journal of Applied Polymer Science:* 2123-2138

Katzbauer, B. 1998. Properties and applications of xanthan gum, Polym. Degrad. Stab. 59 (1–3) : 81–84.

Lakatos, Lakatos-Szabo & Toth, 1981. Factors influencing polyacrylamide adsorption in porous media and their effect on flow behavior. Surface Phenomena in Enhanced Oil Recovery, pp. 821-842.

Lee, L. T. and Somasundaran, P. 1989. Adsorption of Polyacrylamide on Oxide Minerals. Langmuir 5 (3): 854–860. https://doi.org/10.1021/la00087a047

Levitt, D., Dufour, S., Pope, G. A., Morel, D. C., and Gauer, P. R., 2011. Design of an ASP flood in a High-Temperature, High-Salinity, Low-Permeability Carbonate. Paper SPE 14915, International Petroleum Technology Conference, Bangkok, Thailand.

Li, K., Jing, X., He, S. et al. 2016. Static Adsorption and Retention of Viscoelastic Surfactant in Porous Media: EOR Implication. Energy Fuels 30 (11): 9089–9096. https://doi.org/10.1021/acs.energyfuels.6b01732

Li, Q., Pu, W., Wei, B., Jin, F., Li, K. 2017. Static adsorption and dynamic retention of an anti-salinity polymer in low permeability sandstone core. State Key Laboratory of Oil and Gas Reservoir Geology and Exploitation, Southwest Petroleum University.

Mandal, A., Kumar, S. R., Bera, A. 2015. Modelling of surfactant and surfactant–polymer flooding for enhanced oil recovery using STARS (CMG) software, J. Pet. Explor. Prod. Technol. 5 (1): 1–11

Mishra, Saurabh & Bera, Achinta. (2014). Effect of Polymer Adsorption on Permeability Reduction in Enhanced Oil Recovery. Journal of Petroleum Engineering. 2014. 1-9

Moffitt, P.D., 1993. Long term production results of polymer treatments in producing wells in western Kansas. J. Pet. Technol., 356–362

Mohsenatabar, F. A., Derakhshan, A., Shadizadeh, S. R. 2018. An investigation into surfactant flooding and alkaline-surfactant-polymer flooding for enhancing oil recovery from carbonate reservoirs: experimental study and simulation, Energy Sources, Part A Recovery, Util. Environ. Eff.: 1–12

Moradi-Araghi, A. and Doe, P. H., 1987. Hydrolysis and Precipitation of Polyacrylamides in Hard Brines at Elevated Temperatures. SPE Reservoir Engineering, 2(2): 189–198.

Mullayev, B., Abitova, A., Saenko, O., Turkpenbayeva, B. 2017. Uzen oil field: Problems and Solutions: 1st Volume: pp 123-184

Needham, R. B., Doe, P. H. 1987. Polymer flooding review, J. Pet. Technol. 39 (12): 1–503.

Qi, Ehrenfried, Koh & Balhoff, 2017. Reduction of Residual Oil Saturation in Sandstone Cores by Use of Viscoelastic Polymers. SPE Journal, 22(2), pp. 447-458.

Quadri, S. M. R., Shoaib, M., Al Sumaiti, A. M. et al. 2015. Screening of Polymers for EOR in High Temperature, High Salinity and Carbonate Reservoir Conditions. Paper presented at the International Petroleum Technology Conference, Doha, Qatar, 6–9 December. IPTC-18436-MS. https://doi.org/10.2523/IPTC-18436-MS

Rashidi, Sandvik, Blokhus & Skauge, 2009. Static and dynamic adsorption of salt tolerant polymers. IOR 2009-15th European Symposium on Improved Oil Recovery, European Association of Geoscientists & Engineers.

Rellegadla, Prajapat & Agrawal, 2017. Polymers for enhanced oil recovery: fundamentals and selection criteria. Applied Microbiology and Biotechnology, 101(11), pp. 4387-4402.

Saleh, Laila Dao, Wei, Mingzhen , and Baojun Bai. "Data Analysis and Updated Screening Criteria for Polymer Flooding Based on Oilfield Data." SPE Res Eval & Eng 17 (2014): 15–25. doi: https://doi.org/10.2118/168220-PA

Seright, R. S., Campbell, A., Mozley, P., and Han, P., 2010. Stability of Partially Hydrolyzed Polyacrylamides at Elevated Temperatures in the Absence of Divalent Cations. SPE Journal, 15(2): 341–348.

Sheng, J. J. 2011. Modern Chemical Enhanced Oil Recovery: Theory and Practice, first edition. Kidlington, UK: Gulf Professional Publishing.

Sheng, J., 2010. Modern Chemical Enhanced Oil Recovery, pp 130-132, 150-159 (Gulf Professional Publishing is an imprint of Elsevier, Oxford, UK).

Sheng, J., Leonhardt, B., and Azri, N., 2015. Status of Polymer-Flooding Technology, Journal of Canadian Petroleum Technology: 117-119.

Sorbie, K. S., 1991. Polymer-Improved Oil Recovery, first edition, pp 241-253 (CRC Press, Inc. Boca Raton, Florida, USA)

Sorbie, K.S., Collins, I.R., 2010. A proposed pore-scale mechanism for how low salinity waterflooding works. Presented at the SPE Improved Oil Recovery Symposium, Tulsa, 24–28 April.

Sparke, S. J., Kislyakov, P. Y., & Amirtayev, M. A. (2005, June). Significant Production Enhancement in Uzen Field, Kazakhstan through Surface and Subsurface Optimization (SPE94360). In 67th EAGE Conference & Exhibition (pp. cp-1). European Association of Geoscientists & Engineers.

Speight, J. G. 2019. Nonthermal Methods of Recovery: Chapter 2. Heavy Oil Recovery and Upgrading, Gulf Professional Publishing: 49-112.

Szabo, M.T., 1975. Some aspects of polymer retention in porous media using a 14C-tagged hydrolyzed polyacrylamide, pp 323-337, (SPEJ).

Thomas, A. 2016. Polymer Flooding: Chapter 2.INTECH: Open Science, Open Minds. : 57-62

Ulmishek, G. F. 1990. Uzen Field--USSR Middle Caspian Basin, South Mangyshlak Region.

Willhite, G. P. 1986. Waterflooding, Vol. 3, pp 17-23, (Textbook Series, SPE, Texas).

Willhite, G.P., Dominguez, J.G., 1977. Mechanisms of polymer retention in porous media, pp 511-554, (Improved Oil Recovery by Surfactant and Polymer Flooding. Academic Press).

Willhite, G.P., Uhl, J.T., 1988. Correlation of the mobility of biopolymer with polymer concentration and rock properties in sandstone, pp 577, Proceedings of the ACS Division of PMSE Fall Meeting, Anaheim.

Zaitoun, A. and Potie, B., 1983. Limiting Conditions for the Use of Hydrolyzed Polyacrylamides in Brines Containing Divalent Ions. Paper SPE 11785, SPE Oilfield and Geothermal Chemistry Symposium, Denver, Colorado, USA.

Zhang, Guoyin & Seright, 2014. Effect of concentration on HPAM retention in porous media. s.l., SPE Annual Technical Conference and Exhibition.

Zhao, F.-L., 1991. Chemistry in Oil Production, (University of Petroleum, China).

Zheng, et al., 1998. Effects of polymer adsorption and flow behaviour on two-phase flow in porous. Tulsa, SPE/DOE Improved Oil Recovery Symposium.